

Social learning strategies regulate the wisdom and madness of interactive online crowds

Wataru Toyokawa^{1,2,3,†}, Andrew Whalen⁴, and Kevin N. Laland¹

¹*School of Biology, University of St Andrews, Harold Mitchel Building, St Andrews, Fife, KY16 9TH, Scotland*

²*Japan Society for the Promotion of Science, Kojimachi, Chiyoda-ku, Tokyo, 102-0083, Japan*

³*Department of Evolutionary Studies of Biosystems, School of Advanced Sciences, SOKENDAI (The Graduate University for Advanced Studies), Shonan Village, Hayama, Kanagawa 240-0193, Japan*

⁴*The Roslin Institute, University of Edinburgh, Midlothian, SCT, EH25 9RG, Scotland*

[†]*e-mail address: wt25@st-andrews.ac.uk*

1

Abstract

2

3

4

5

6

7

8

9

10

11

12

13

14

15

16

Decentralised social interactions can generate swarm intelligence, but may concurrently increase the risk of maladaptive herding. Here we present an individual-based model analysis suggesting that the conflict between the ‘wisdom’ and ‘madness’ of interactive crowds is regulated by selectively choosing which social learning strategy to use. We used an interactive online experiment with 699 participants to measure the patterns of human social-information use, varying both task uncertainty and group size. Hierarchical Bayesian analyses identified the individual learning strategies, revealing that conformity bias increased with the task’s uncertainty, whereas reliance on social learning increased with group size. Mapping individual strategies onto collective behaviour, we show that maladaptive herding occurred more frequently when larger groups were engaged in more uncertain tasks. Our computational modelling approach provides novel evidence that the likelihood of swarm intelligence versus herding can be predicted using knowledge of social learning strategies. (currently 144 words)

Keywords: swarm intelligence, herding, social learning, computational modelling, web-based experiment, hierarchical Bayesian approach

17 **1 Introduction**

18 Understanding the mechanisms that account for accurate collective decision-making amongst
19 groups of animals has been a central focus of animal behaviour research (Bonabeau et al., 1999;
20 Camazine et al., 2001; Sumpter, 2010). There are a large number of biological examples showing
21 that collectives of poorly informed individuals can achieve a high performance in solving cog-
22 nitive problems under uncertainty (Krause et al., 2010). Examples of such ‘swarm intelligence’
23 – the emergent wisdom of interactive crowds – have been found in a broad range of biological
24 systems (Table 1). Although these findings suggest fundamental cognitive benefits of grouping
25 (Krause and Ruxton, 2002), there is also a long-standing recognition, especially for humans, that
26 interacting individuals may sometimes be overwhelmed by the ‘*extraordinary popular delusions*
27 *and madness of crowds*’ (Mackay, 1841). Herd behaviour (i.e. an alignment of thoughts or be-
28 haviours of individuals in a group) occurs because individuals imitate each others (Kameda and
29 Hastie, 2015; Le Bon, 1896; Raafat et al., 2009), and it is thought to be a cause of financial
30 bubbles (Chari and Kehoe, 2004; Mackay, 1841), ‘groupthink’ (Janis, 1972) and volatility in
31 cultural markets (Muchnik et al., 2013; Salganik et al., 2006). More generally, herding is known
32 to undermine the wisdom of crowds effect (Lorenz et al., 2011), whilst maladaptive aspects of
33 information transfer are well-recognised in the biological literature (e.g. Giraldeau et al., 2002).
34 It seems that information transmission among individuals, and making decisions collectively, is
35 a double-edged sword: combining decisions may provide the benefits of swarm intelligence, but
36 at the same time, increase the risk of maladaptive herding. Collectively, an understanding of
37 whether and, if so, how it is possible to prevent or reduce the risk of maladaptive herd behaviour,

38 while concurrently keeping or enhancing swarm intelligence, is largely lacking.

Table 1

Examples of swarm intelligence in diverse biological systems

Taxonomic families	Examples and references
Slime moulds	Finding conditions favorable to spore survival and dispersal (Reid and Latty, 2016)
Social insects	Collective foraging (Seeley et al., 1991; Shaffer et al., 2013) and nest-site selection (Franks et al., 2003; Sasaki and Pratt, 2012; Sasaki et al., 2013; Seeley and Visscher, 2004)
Fish	Collective sensing (Berdahl et al., 2013; Sumpter et al., 2008), predator avoidance (Ward et al., 2011) and foraging decisions (Webster et al., 2017)
Birds	Collective foraging (Liker and Bokony, 2009; Morand-Ferron and Quinn, 2011) and homing decisions (Sasaki and Biro, 2017)
Non-human primates	Group coordination in where and when to move (King and Sueur, 2011)
Humans	Decision-making in an estimation task (Krause et al., 2011; Rosenberg and Pescetelli, 2017) and in a multi-armed bandit task (Toyokawa et al., 2014)

39 A balance between using individual and social information may play a key role in determining
40 the trade-off between collective wisdom and maladaptive herding (List et al., 2009). If individu-
41 als are too reliant on copying others' behaviour, any ideas, even a maladaptive one, can propagate
42 in the social group (i.e. the 'informational cascade'; Bikhchandani et al., 1992; Giraldeau et al.,
43 2002; Richerson and Boyd, 2005). On the other hand, however, if individuals completely ignore

44 social information so as to be independent, they will fail to exploit the benefits of aggregating
45 information through social interactions. The extent to which individuals should use social in-
46 formation should fall between these two extremes. Theoretical models predict that the balance
47 between independence and interdependence in collective decision-making may be changeable,
48 contingent upon the individual-level flexibility and inter-individual variability associated with
49 the social learning strategies deployed in diverse environmental states (e.g. Arbilly et al., 2011;
50 Boyd and Richerson, 1985; Feldman et al., 1996; Laland, 2004).

51 Animals (including humans) are reported to increase their use of social information as re-
52 turns from asocial learning become more unreliable (e.g. Kameda and Nakanishi, 2002; Kendal
53 et al., 2004; Morgan et al., 2012; Toyokawa et al., 2017; Webster and Laland, 2008, 2011). In
54 addition, individuals are predicted to be more likely to rely on social learning larger the number
55 of individuals that share information (Boyd and Richerson, 1989; Bond, 2005; Kline and Boyd,
56 2010; Morgan et al., 2012; Muthukrishna et al., 2014; Street et al., 2017). This selectivity in the
57 predicted use of social information may have a substantial impact on collective decision-making
58 because only a slight difference in the parameter values of social information use is known to
59 be able to alter qualitatively the collective behavioural dynamics (e.g. Bonabeau et al., 1999;
60 Camazine et al., 2001; Nicolis and Deneubourg, 1999; Pratt and Sumpter, 2006). Therefore, re-
61 searchers should expect populations to exhibit a higher risk of being trapped with maladaptive
62 behaviour with increasing group size and decreasing reliability of asocial learning (and concomi-
63 tant increased reliance on social learning).

64 From the viewpoint of the classic wisdom of crowds theory, increasing group size may in-
65 crease collective accuracy (List, 2004; King and Cowlshaw, 2007; Wolf et al., 2013; Becker

66 et al., 2017; Laan et al., 2017). The relative advantage of the collective over solitary individuals
67 may also be highlighted by increased task difficulty, because there would be more room in the
68 performance to be improved compared to easier tasks in which high accuracy can already be
69 achieved by asocial learning only (Cronin, 2016). To understand the potential conflict between
70 swarm intelligence and the risk of maladaptive herding requires fine-grained quantitative studies
71 of social learning strategies and their relations to collective dynamics, linked to sophisticated
72 computational analysis.

73 The aims of this study were twofold. First, we set out to examine whether altering both the
74 reliability of asocial learning and group size would induce heavier use of social information in
75 humans, and thereby alter the balance between swarm intelligence and the risk of maladaptive
76 herding. To do this, we focused on human groups exposed to a simple gambling task, where
77 both asocial and social sources of information were available. Second, we sought to conduct a
78 detailed analysis of the complex relationship between individual-level decision, learning strate-
79 gies and population-level behavioural outcomes. Our use of an abstract decision-making task
80 allowed us to implement a computational modelling approach, which has been increasingly de-
81 ployed in quantitative studies of animal social learning strategies (Ahn et al., 2014; Aplin et al.,
82 2017; Barrett et al., 2017; McElreath et al., 2005, 2008; Toyokawa et al., 2017). In particular,
83 computational modelling allowed us to conduct a parametric description of different information-
84 gathering processes and to estimate these parameter values at an individual-level resolution.

85 Below, we firstly described our experimental task and summarise the computational model.
86 Then, we deploy agent-based simulation to illustrate how the model parameters relating to social
87 learning can in principle affect the collective-level behavioural dynamics. The simulation pro-

88 vides us with precise, quantitative predictions on the complex relationship between individual
89 behaviour and group dynamics. Finally, we present the findings of a multi-player web-based ex-
90 periment with human participants that utilises the gambling task framework. Applying a hierar-
91 chical Bayesian statistical method, we estimated the model's parameters for each of 699 different
92 individuals, allowing us to (i) examine whether and, if so, how social information use is affected
93 by different group size and task uncertainty, and (ii) whether and how social-information use
94 affects the balance between swarm intelligence and maladaptive herding.

95 **1.1 Task overview**

96 To study the relationship between social information use and collective behavioural dynamics, we
97 focused on a well-established learning-and-decision problem called a 'multi-armed bandit' task,
98 represented here as repeated choices between three slot machines (Figure S1, Video 1, for detail
99 see Materials and methods). Individuals play the task for 70 rounds. The slots paid off money
100 noisily, varying around two different means during the first 40 rounds such that there was one
101 'good' slot and two other options giving poorer average returns. From the round 41st, however,
102 one of the 'poor' slots abruptly increased its mean payoff to become 'excellent' (i.e. superior
103 to 'good'). The purpose of this environmental change was to observe the effects of maladaptive
104 herding by potentially trapping groups in the out-of-date suboptimal (good) slot, as individuals
105 did not know whether or how an environmental change would occur. Through making choices
106 and earning a reward from each choice, individuals could gradually learn which slot generated
107 the highest rewards.

108 In addition to this asocial learning, we provided social information for each member of the

109 group specifying the frequency with which group members chose each slot. All group mem-
110 bers played the same task with the same conditions simultaneously, and all individuals had been
111 instructed that this was the case, and hence understood that the social information would be in-
112 formative.

113 Task uncertainty was experimentally manipulated by changing the difference between the
114 mean payoffs for the slot machines. In the task with the least uncertainty, the distribution of
115 payoffs barely overlapped, whilst in the task with the greatest uncertainty the distribution of
116 payoffs overlapped considerably (Figure S3).

117 1.2 Overview of the computational learning-and-decision-making model

118 We modelled individual behavioural processes by assuming that individual i makes a choice for
119 option m at round t , in accordance with the choice-probability $P_{i,t}(m)$ that is a weighted average
120 of social and asocial influences:

$$P_{i,t}(m) = \sigma_{i,t} \times \text{Social influence}_{i,m,t} + (1 - \sigma_{i,t}) \times \text{Asocial influence}_{i,m,t}, \quad (1)$$

121 where $\sigma_{i,t}$ is the *social learning weight* ($0 \leq \sigma_{i,t} \leq 1$).

122 For the social influence, we assumed a frequency-dependent copying strategy by which an
123 individual copies others' behaviour in accordance with the distribution of social frequency infor-
124 mation (McElreath et al., 2005, 2008; Aplin et al., 2017; Barrett et al., 2017):

$$\text{Social influence}_{i,m,t} = \frac{\left(\text{frequency}_{m,t-1}\right)^{\theta_i}}{\sum_{k \in \text{options}} \left(\text{frequency}_{k,t-1}\right)^{\theta_i}}, \quad (2)$$

125 where $frequency_{m,t-1}$ is a number of choices made by other individuals for the option m in the
126 preceding round $t - 1$ ($t \geq 2$). The exponent θ_i is individual i 's *conformity exponent* ($-\infty \leq$
127 $\theta_i \leq +\infty$). When this exponent is larger than zero ($\theta_i > 0$), higher social influence is afforded to
128 an option chosen by more individuals (i.e. positive frequency bias), with conformity bias arising
129 when $\theta_i > 1$, such that disproportionately more social influence is given to the most common
130 option (Boyd and Richerson, 1985). When $\theta_i < 0$, on the other hand, higher social influence is
131 afforded to the option that fewest individuals chose in the preceding round $t - 1$ (i.e. negative
132 frequency bias). Note, there is no social influence when $\theta_i = 0$ because in this case the 'social
133 influence' favours an uniformly random choice, i.e., $Social\ influence_{i,m,t} = f_m^0 / (f_1^0 + f_2^0 + f_3^0) =$
134 $1/3$, independent of the social frequency distribution.

135 For the asocial influence, we used a standard 'softmax' choice rule well-established in the
136 reinforcement-learning literature (Sutton and Barto, 1998) and widely applied in human social
137 learning studies (e.g. McElreath et al., 2005, 2008; Toyokawa et al., 2017).

138 In summary, the model has two key social learning parameters, the *social learning weight* $\sigma_{i,t}$
139 and the *conformity exponent* θ_i , with $\sigma_{i,t}$ a time-dependent variable (i.e. individuals could modify
140 their reliance on social learning as the task proceeded). Varying these parameters systematically,
141 we conducted an individual-based simulation so as to establish quantitative predictions concern-
142 ing the relationship between social information use and collective behaviour. We then fitted this
143 model to our experimental data using a hierarchical Bayesian approach. This method allows
144 us to specify with precision how each individual subject learns (i.e. which learning strategy or
145 strategies they deploy), and thereby to describe the range and distribution of learning strategies
146 deployed across the sample, and to investigate their population-level consequences.

147 **2 Results**

148 **2.1 The relationship between social information use and the collective behaviour**

149 Figure 1 shows the relationship between the average decision accuracy and individual-level social
150 information use obtained from our individual-based model simulations. Figure 1a and 1c show
151 that individuals in larger groups perform better both before and after the environmental change
152 when the mean conformity exponent $\bar{\theta}$ is small (i.e. $\bar{\theta} = (\sum_i \theta_i)/individuals = 1$). In the
153 absence of conformity, even when the average social learning weight is very high (i.e. $\bar{\sigma} =$
154 $(\sum_i \sum_t \sigma_{i,t})/(individuals \times rounds) = 0.9$), larger groups are still able to recover the decision
155 accuracy after the location of the optimal option has been switched.

156 On the other hand, when the mean conformity exponent is large (i.e. $\bar{\theta} = 3$; strong confor-
157 mity bias), the group dynamics become less flexible, and become vulnerable to getting stuck on
158 a suboptimal option after environmental change. Here, the recovery of performance after envi-
159 ronmental change takes more time in larger compared to smaller groups (Figure 1b). When both
160 the conformity exponent $\bar{\theta}$ and the social learning weight $\bar{\sigma}$ are large (Figure 1d), performance
161 is no longer monotonically improving with increasing group size, and it is under these circum-
162 stances that the strong herding effect becomes prominent. Figure 2c and 2d indicate that when
163 both $\bar{\theta}$ and $\bar{\sigma}$ are large the collective choices converged either on the good option or on one of the
164 poor options almost randomly, regardless of the option's quality, and that once individuals start
165 converging on an option the population gets stuck. As a result, the distribution of the groups'
166 average performance over the replications becomes a bimodal 'U-shape'. Interestingly, however,
167 the maladaptive herding effect remains relatively weak in smaller groups (see Figure 2c; the black

168 histograms). This is because the majority of individuals in smaller groups (i.e. two individuals
169 out of three) are more likely to break the cultural inertia by simultaneously exploring for another
170 option than the majority in larger groups (e.g. six out of ten). As expected, herding does not
171 occur in the absence of conformity (Figure 2a, 2b).

172 In summary, the model simulation suggests an interaction between social learning weight $\bar{\sigma}$
173 and conformity exponent $\bar{\theta}$ on decision accuracy and the risk of maladaptive herding: When the
174 conformity exponent is not too large, swarm intelligence is prominent across a broad range of
175 the mean social learning weights (i.e. increasing group size can increase decision accuracy while
176 concurrently retaining decision flexibility). When the conformity bias becomes large, however,
177 the risk of maladaptive herding arises, and, when both social learning parameters are large, swarm
178 intelligence is rare and maladaptive herding dominates.

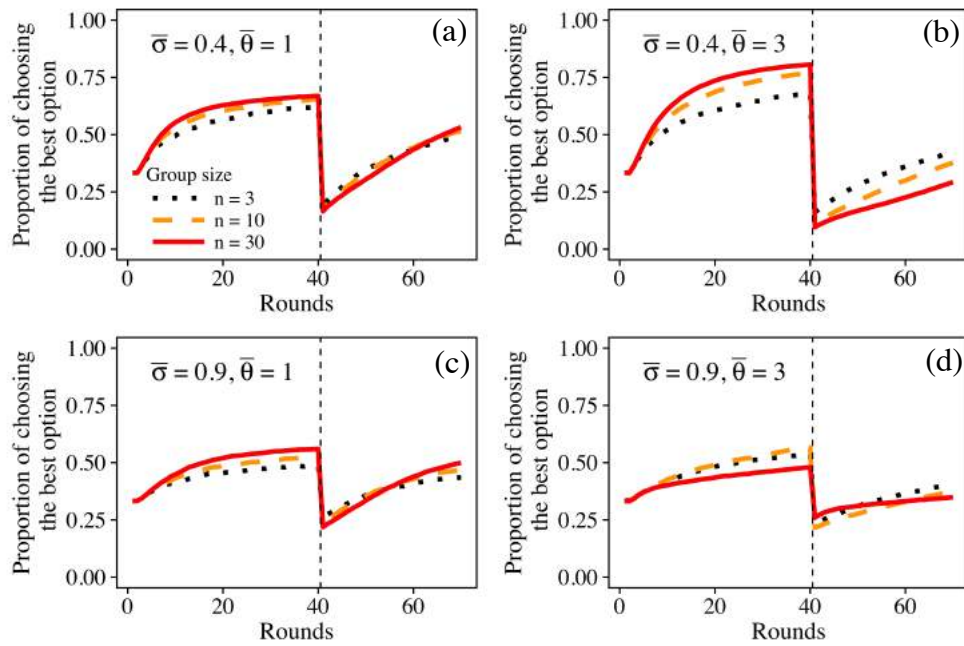


Figure 1: Findings of the individual-based model showing the effects of social information use on the average decision accuracy over replications. The x-axis gives the round and y-axis gives the proportion of individuals expected to choose the optimal slot (i.e. decision accuracy) averaged over all replications. The vertical dashed line indicates the timing of environmental (i.e. payoff) change (at $t = 41$). Different group sizes are shown by different styles (black (dotted): $n = 3$, orange (dashed): $n = 10$, red (solid): $n = 30$). We set the average slopes for the *social learning weight* to be equal to zero for the sake of simplicity; namely, $\mu_\delta = 0$. Other free parameter values (i.e. μ_α , $\mu_{\beta_0^*}$, μ_ϵ , v_α , $v_{\beta_0^*}$, v_ϵ , v_σ , v_δ and v_θ) are best approximates to the experimental fitted values (see Table 2 and Table S1).

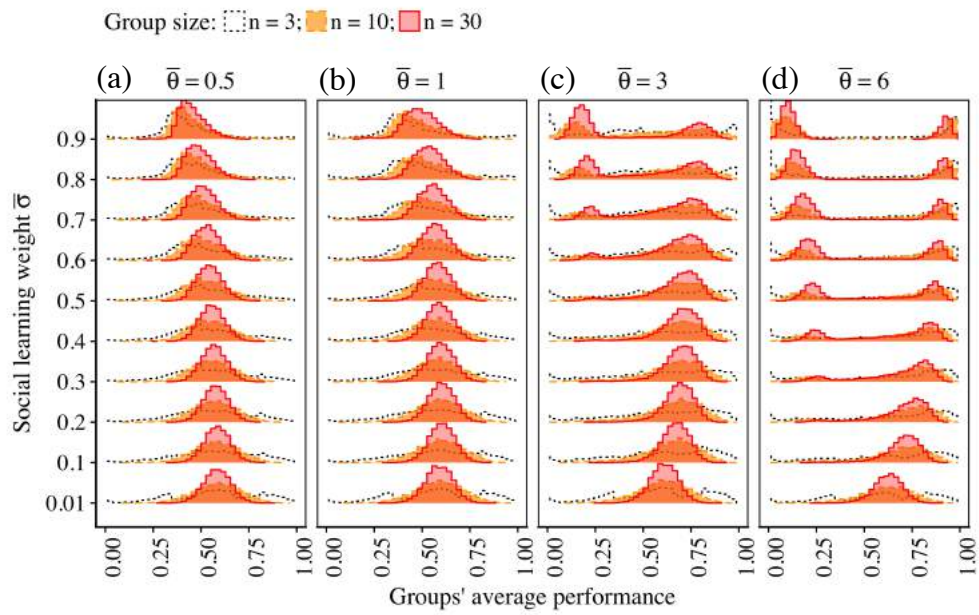


Figure 2: Results from the individual-based model simulations showing the distribution of each group's mean accuracy before environmental change. The x-axis gives the mean decision accuracy over the first 40 rounds (i.e. the environment 1) for each replication. Different group sizes are shown by different styles (black (dotted): $n = 3$, orange (dashed): $n = 10$, red (solid): $n = 30$). Again, $\mu_\delta = 0$, and other free parameter values (i.e. μ_α , $\mu_{\beta_0^*}$, μ_ϵ , ν_α , $\nu_{\beta_0^*}$, ν_ϵ , ν_σ , ν_δ and ν_θ), we approximated using experimental data (see Table 2 and Table S1).

179 **2.2 Estimation of human social information use**

180 Table 2 reveals how the *social learning weight* $\sigma_{i,t}$ and *conformity exponent* θ_i were influenced
181 by task uncertainty in our behavioral experiment. It gives posterior estimation values for each of
182 the global means of the learning model parameters, obtained by the hierarchical Bayesian model
183 fitting method applied to the experimental data (see the Materials and methods). The fitted global
184 variance parameters (i.e. v) are shown in the Supporting Table S1.

Table 2

The mean and the 95% Bayesian credible intervals of the posterior global means for the parameter values. The number of participants (N) for each experimental condition are also shown.

Parameters	Group condition				Solitary condition			
	Uncertainty				Uncertainty			
	Low	Moderate	High	Low	Moderate	High	Moderate	High
μ_{α^*} (learning rate)	0.99 [0.34, 1.73]	0.90 [0.43, 1.44]	0.61 [0.21, 1.03]	0.85 [-0.07, 1.95]	-0.17 [-1.27, 0.89]	0.46 [-0.39, 1.36]		
$\mu_{\beta_0^*}$ (inv. temp.)	1.84 [1.15, 2.70]	1.68 [1.25, 2.18]	1.38 [1.16, 1.62]	1.10 [0.69, 1.54]	1.44 [0.80, 2.07]	0.85 [0.46, 1.22]		
μ_{ϵ} (inv. temp.)	3.70 [1.98, 5.71]	3.01 [1.88, 4.27]	2.97 [2.37, 3.60]	2.39 [1.46, 3.53]	2.81 [1.64, 4.07]	2.27 [1.40, 3.31]		
$\mu_{\sigma_0^*}$ (soc. wight)	-1.55 [-2.71, -0.71]	-2.37 [-4.12, -1.01]	-2.16 [-2.81, -1.63]	-	-	-	-	-
μ_{δ} (soc. wight)	-1.39 [-2.66, -0.03]	-1.55 [-4.29, 0.91]	-1.87 [-3.04, -0.81]	-	-	-	-	-
μ_{θ} (conformity coeff.)	1.65 [0.83, 2.82]	3.00 [1.57, 4.85]	2.67 [1.80, 3.73]	-	-	-	-	-
N	77	98	398	36	34	56		

185 We were able to categorize the participants as deploying three different learning strategies
186 based on their fitted conformity exponent values; namely, the ‘positive frequency-dependent
187 copying’ strategy ($\theta_i \gg 0$), the ‘negative-frequency dependent copying’ strategy ($\theta_i \ll 0$) and
188 the ‘random choice’ strategy ($\theta_i \approx 0$). Note that we could not reliably detect the ‘weak positive’
189 frequency-dependent strategy ($0 < \theta_i \leq 1$) due to the limitation of statistical power (Figure S10
190 and S17). Some individuals whose ‘true’ conformity exponent fell between zero and one would
191 have been categorised as exhibiting a random choice strategy (Figure S10). Individuals identi-
192 fied as exhibiting a positive frequency-dependent copiers were mainly those whose conformity
193 exponent was larger than one ($\theta_i > 1$).

194 Figure 3a-c show the estimated frequencies of different learning strategies. Generally speak-
195 ing, participants were more likely to utilize a positive frequency-dependent copying strategy
196 than the other two strategies (the 95% Bayesian CI of the intercept of the GLMM predicting the
197 probability to use the positive frequency-dependent copying strategy is above zero, [1.05, 2.50];
198 Table S2). We found that positive frequency-dependent copying decreased with increasing task
199 uncertainty (the 95% Bayesian CI of task uncertainty effect is below zero, [-1.88, -0.25]; Table
200 S2). We found no clear effects of either the group size, age or gender on adoption of the positive
201 frequency-dependent copying strategy, except for the negative interaction effect between age and
202 task uncertainty (the 95% Bayesian CI of the age \times uncertainty interaction = [-1.46, -0.15]; Table
203 S2).

204 We also investigated the effects of group size and task uncertainty on the fitted individual
205 parameter values. We found that the individual mean *social learning weight* parameter (i.e.
206 $\bar{\sigma}_i = (\sum_t \sigma_{i,t})/70$) increased with group size (the 95% Bayesian CI = [0.15, 0.93]; Figure 3d-f;

207 Table S3), and decreased with uncertainty (the 95% Bayesian CI = [-0.98, -0.22]), and age of
208 subject (the 95% Bayesian CI = [-0.36, -0.02]). However, the negative effects of task uncertainty
209 and age disappeared when we focused only on $\bar{\sigma}_i$ of the positive frequency-dependent copying
210 individuals, and only the positive effect of the group size was confirmed (Table S4; Figure S16).
211 It is worth noting that the meaning of the social learning weight is different between these three
212 different strategies: The social learning weight regulates positive reactions to the majorities' be-
213 haviour for positive frequency-dependent copiers, whereas it regulates avoidance of the majority
214 for negative-frequency dependent copiers, and determines the probability of random decision-
215 making for the random choice strategists.

216 The individual *conformity exponent* parameter θ_i increased with task uncertainty (the 95%
217 Bayesian CI = [0.38, 1.41]), but we found no significant effects of group size, age, gender or
218 interactions (Figure 3g-i; Table S5). These results were qualitatively unchanged when we focused
219 only on the positive frequency-dependent copying individuals (Table S6; Figure S16).

220 We observed extensive individual variation in social information use. The greater the task's
221 uncertainty, the larger were individual variances in both the mean social learning weight and the
222 conformity exponent (the 95% Bayesian CI of the GLMM's variation parameter for $\bar{\sigma}_i$ was [1.11,
223 1.62] (Table S3) and for θ_i was [1.07, 1.54] (Table S5)). This was confirmed when focusing only
224 on the positive frequency-dependent copying individuals: The Bayesian 95% CIs were [1.14,
225 1.80] (Table S4) and [0.71, 1.10] (Table S6), respectively.

226 The manner in which individual variation in social-information use of positive frequency-
227 dependent copying individuals changes over time is visualised in Figure 4a-c. The social learn-
228 ing weights generally decreased with experimental round. However, some individuals in the

229 Moderate- and the High-uncertain conditions accelerated rather than decreased their reliance on
230 social learning over time. Interestingly, those accelerating individuals tended to have a larger
231 conformity exponent (Figure S18). In addition, the time-dependent $\theta_{i,t}$ in our alternative model
232 generally increased with experimental round in the Moderate- and the High-uncertainty condi-
233 tions (see the appendix; Figure S26), although the fitting of $\theta_{i,t}$ in the alternative model was
234 relatively unreliable (Figure S20). These findings suggest that conformists tended to use asocial
235 learning at the outset but increasingly started to conform as the task proceeded.

236 Extensive variation in the temporal dynamics of the social learning weight $\sigma_{i,t}$ was also found
237 for the negative-frequency dependent copying individuals but not found for the random choice
238 individuals (Figure S14). Individuals deploying a random choice strategy exhibited a $\sigma_{i,t}$ that ap-
239 proached to zero, indicating that their decision-making increasingly relied exclusively on asocial
240 reinforcement learning as the task proceeded.

241 No significant fixed effects were found in other asocial learning parameters such as the learn-
242 ing rate α_i and the mean inverse temperature $\bar{\beta}_i = (\sum_t \beta_{i,t})/70$ (Table S7, Table S8 and Figure
243 S15).

244 In summary, our experiments on adult humans revealed asymmetric influences of increasing
245 task uncertainty and increasing group size on the social learning parameters. The conformity
246 exponent increased with task uncertainty on average but the proportion of positive frequency-
247 dependent copying individuals showed a corresponding decrease, due to the extensive individual
248 variation emerging in the High-uncertain condition. Conversely, group size had a positive effect
249 on the mean social learning weight, but did not affect conformity (Figure 3, 4a-c).

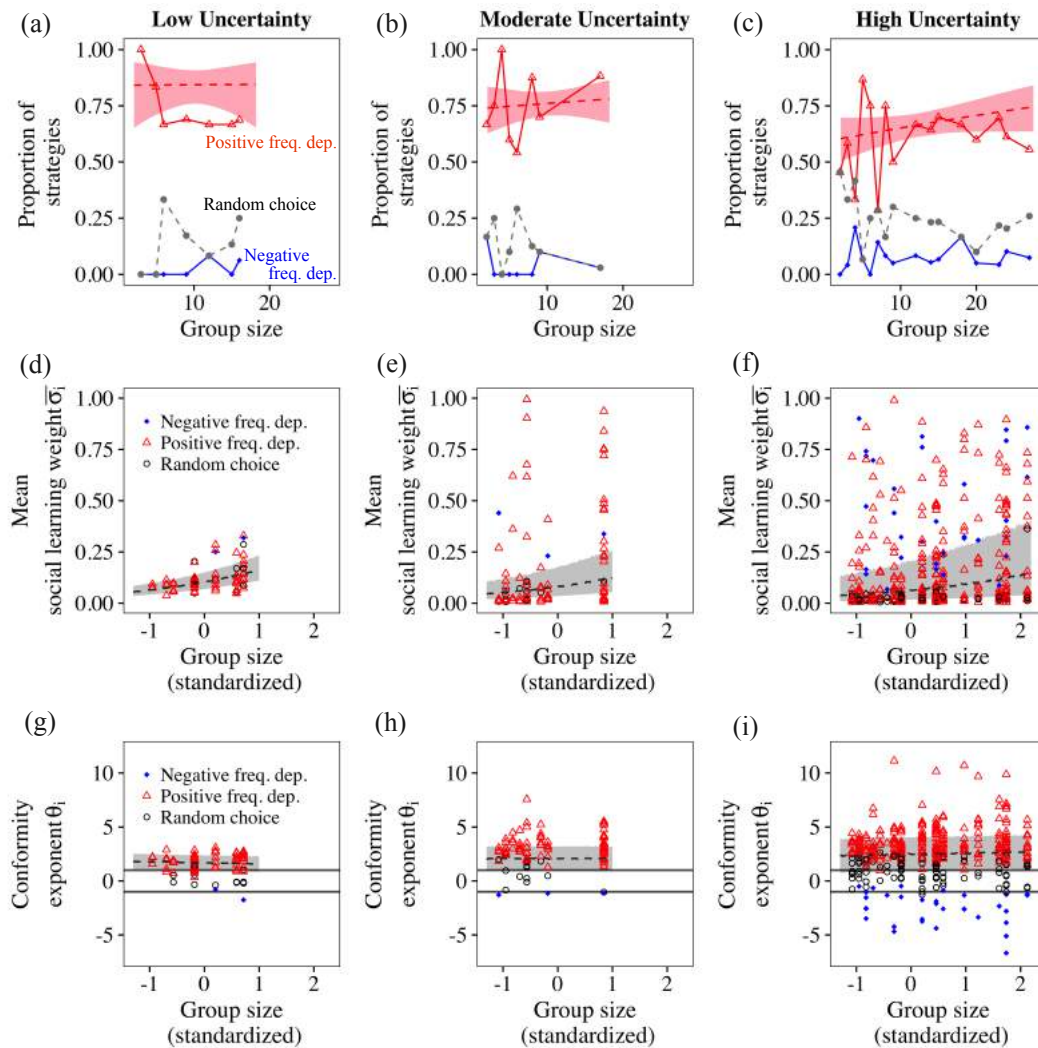


Figure 3: Model fitting for the three different task's uncertain conditions (the Low-, Moderate- and High-uncertainty) and the different group size. Three different learning strategies are shown in different styles (red-triangle: positive frequency-dependent learning, blue-circle: negative frequency-dependent learning; grey-circle: nearly random choice strategy). (a-c) Frequencies of three different learning strategies. Note that a sum of the frequencies of these three strategies in the same group size does not necessarily equal to 1, because there are a small number of individuals eliminated from this analysis due to insufficient data. (d-f) Estimated social learning weight, and (g-i) estimated conformity exponent, for each individual shown for each learning strategy. The 50% Bayesian CIs of the fitted GLMMs are shown by dashed lines and shaded areas. The horizontal lines in (g-i) show a region $-1 < \theta_i < 1$.

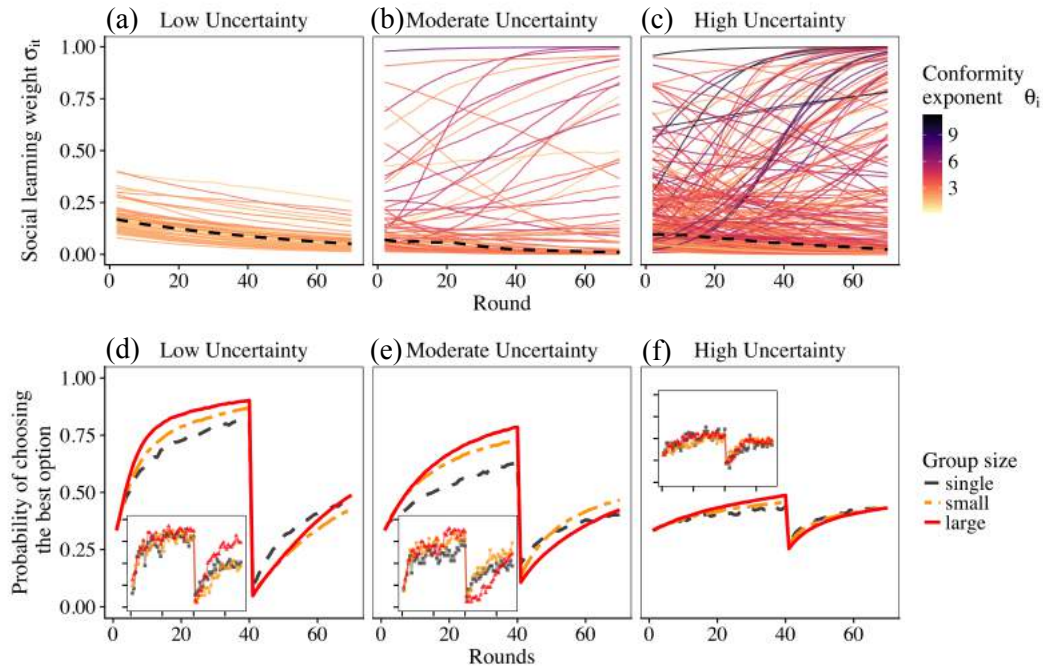


Figure 4: (a-c) Change in fitted values (i.e. median of the Bayesian posterior distribution) of the social learning weight $\sigma_{i,t}$ with time for each individual, for each level of task uncertainty. Thick dashed lines are the median values of $\sigma_{i,t}$ across the subjects for each uncertainty condition. Individual conformity exponent values θ_i are shown in different colours (higher θ_i is darker). (d-f) Change in average decision accuracy of the individual-based post-hoc model simulations using the experimentally fit parameter values (main panels). The inner panels show the average decision accuracies of the experimental participants. Each line indicates different group-size categories (red-solid: large groups, orange-halfdashed: small groups, grey-dashed: lone individuals). All individual performances were averaged within the same size category. The large or small groups were categorised using the median sizes for each experimental condition, i.e. small groups were: $n \leq 9$, $n \leq 6$ and $n \leq 11$ for the Low-, Moderate- and High-uncertain conditions, respectively.

250 **2.3 A balance between the collective decision accuracy and the herding effect**

251 Figure 4d-f show the change over time in performance with different group sizes and different
252 uncertainty conditions, generated by the post-hoc simulations of the parameter-fitted model. The
253 mean decision accuracies of the experimental groups are shown in the inner windows. Because
254 the post-hoc simulations were run for 5,000 replications for each group size, which should gen-
255 erate more robust pattern than the raw experimental data basing only on a limited number of
256 experimental replications, and given the correspondence between simulations and data, below
257 we concentrate our interpretation on the simulated results.

258 Prior to the environmental change (Round 1 to 40), larger groups performed better on average
259 than did both smaller groups and lone individuals across all the uncertainty levels, suggesting
260 swarm intelligence was operating. However, after the environmental change (i.e. from Round 41)
261 performance differed between the conditions. In the Low-uncertain condition, where we found
262 that the participants were most likely to have a relatively weak positive frequency-dependence
263 (i.e. $\bar{\theta} = 1.65$), large groups again made more accurate decisions than small groups (Figure 4d,
264 from Round 41). However, in the Moderate- and the High-uncertain condition, where we found
265 that participants were most likely to have strong positive frequency dependence ($\bar{\theta} = 3.00$ and
266 2.67, c.f. 1.65 in the Low-uncertainty condition), the large groups seemed to get stuck on the
267 suboptimal option after the change (Figure 4e and 4f, from Round 41), although the decision
268 accuracy did not substantially differ with group size in the High-uncertain condition.

269 Lone individuals in the Low-uncertain condition recovered performance more quickly than
270 did both the small and large groups even though the lone individuals performed worse in the first-
271 half of the task (Figure 4d), suggesting that asocial learners are more capable of detecting the

272 environmental change than individuals in groups. This might be due to the higher exploration rate
273 of lone individuals (both $\mu_{p_0^*}$ and μ_e of solitary individuals were smaller than those of grouping
274 individuals; Table 2).

275 Overall, the pattern of results was broadly consistent with our predictions (Figure 1). We
276 confirmed that in the Low-uncertainty condition, where individuals have weaker positive fre-
277 quency bias, larger groups were more accurate than smaller groups while retaining flexibility
278 in their decision-making (i.e. swarm intelligence dominates). However, in the Moderate- and
279 the High-uncertain conditions, larger groups performed better prior to environmental change but
280 were vulnerable to getting stuck with an out-dated maladaptive option due to the larger estimated
281 conformity exponent, thereby generating the conflict between swarm intelligence and maladap-
282 tive herding.

283 **3 Discussion**

284 We investigated whether and how human social learning strategies regulate the conflict between
285 swarm intelligence and herding behaviour using a collective learning-and-decision-making task
286 combined with simulation and model fitting. We examined whether manipulating the reliability
287 of asocial learning and group size would affect the use of social information, and thereby alter the
288 collective decision dynamics, as suggested by our computational model simulation. Although a
289 theoretical study has suggested that reliance on social learning and conformity bias would play a
290 role in collective dynamics (Kandler and Laland, 2013), thus far no empirical studies have quan-
291 titatively investigated the population-level consequences of these two different social learning
292 processes. Our high-resolution, model-based behavioural analysis using a hierarchical Bayesian

293 statistics enabled us to identify individual-level patterns and variation of different learning pa-
294 rameters and to explore their population-level outcomes. The results provide strong support for
295 our hypothesis that the conflict between the swarm intelligence effect and maladaptive herding
296 can be predicted with knowledge of human social learning strategies.

297 Consistent with previous empirical findings (e.g., Morgan et al., 2012; Muthukrishna et al.,
298 2014), adult human participants were increasingly likely to make a conformity-biased choice as
299 the uncertainty of the task went up (i.e. as it became more difficult to determine the best option.
300 Figure 3g-i). The fitted global mean values of the conformity exponent parameters were 3.0 and
301 2.7 in the Moderate- and the High-uncertain conditions, respectively (Table 2), and these values
302 were sufficiently high to cause larger populations to get stuck on a suboptimal option following
303 environmental change (Figure 1b; Figure 4e, 4f). Conversely, in the Low-uncertain condition
304 individuals exhibited relatively weak conformity (i.e. $\bar{\theta} \approx 1.65$), allowing larger groups to escape
305 the suboptimal option, and retain their swarm intelligence (Figure 1a; Figure 4d). Although
306 the social learning weight was also found to be contingent upon the environmental factors, the
307 estimated mean value was $\bar{\sigma}_i = 0.3$ (Figure 3d-f; Figure S14). This implies a weaker social
308 than asocial influence on decision-making as reported in several other experimental studies (e.g.
309 Efferson et al., 2008; McElreath et al., 2005; Mesoudi, 2011; Toyokawa et al., 2017). Thanks to
310 this relatively weak reliance of social learning, the kind of herding that would have blindly led a
311 group to any option regardless of its quality (like the ‘symmetry breaking’ known in social insect
312 collective foraging systems. Figure 2c,d; Camazine et al., 2001; Sumpter, 2010), did not occur.
313 Research that explores the factors that can induce higher social learning weights in humans,
314 in order to understand under which circumstances herd behaviour would dominate, would be

315 valuable.

316 Individual differences in exploration might also play a crucial role in shaping collective de-
317 cision dynamics. Although a majority of participants adopted a positive frequency-dependent
318 copying strategy, some individuals exhibited negative frequency dependent or random decision-
319 making strategy (Figure 3a-c). It is worth noting that the random choice strategy was associated
320 with more exploration than the other strategies, because it led to an almost random choice at a
321 rate σ_i , irrespective of the options' quality. In addition, negative-frequency dependent copying
322 individuals could also be highly exploratory. These individuals tended to avoid choosing an op-
323 tion upon which the other people had converged and would explore the other two 'unpopular'
324 options. Interestingly, in the High-uncertain condition the mean social learning weights of the
325 negative-frequency dependent copying individuals ($\bar{\sigma}_i \approx 0.5$) were larger than that of the other
326 two strategies ($\bar{\sigma}_i \approx 0.1$, Figure S14), indicating that these individuals engaged in such majority-
327 avoiding exploration relatively frequently. Such high exploratory tendencies would prevent in-
328 dividuals from converging on a better option, leading to a diminishing of swarm intelligence in
329 high-uncertainty circumstances (Figure 4f).

330 Individual differences have received increasing attention in both collective behaviour and
331 animal social learning studies (e.g. Jolles et al., 2018; Michelena et al., 2010; Planas-sitja et al.,
332 2015), and across the human behavioural sciences (e.g. Gray et al., 2017; Mesoudi et al., 2016).
333 Our finding that the effects of individual variation depend on uncertainty implies that human
334 subjects' use of social learning strategies is deployed plastically, and is not a fixed propensity (i.e.
335 personality trait), that differs rigidly between individuals (Dingemanse et al., 2010; Toyokawa
336 et al., 2017). Our approach of combining with individual-based simulation and experimentation

337 could potentially prove a powerful tool with which to explore decision-making in other animals.

338 Another methodological advantage of using computational models to study social learn-
339 ing strategies is its explicitness of assumptions about the temporal dynamics of behaviour. It
340 has been argued that just observing the final frequencies of learned behaviour does not provide
341 enough information to determine what asocial and/or social learning processes might have been
342 used because multiple learning-and-decision mechanisms are equally likely to produce the same
343 population-level patterns (Barrett, 2018; Hoppitt and Laland, 2013). For example, very exploita-
344 tive asocial reinforcement learners (i.e. exploitation parameter $\beta_{i,t}$ is large and the social learning
345 weight $\sigma_{i,t}$ is nearly zero) and conformity-biased social learners (conformity exponent θ_i is large
346 and $\sigma_{i,t}$ is positive) would eventually converge on the same option, resulting in the same final
347 behavioural steady state. However, how they explored the environment, as well as how they re-
348 acted to the other individuals in the same group, are significantly different and they could produce
349 qualitatively different collective temporal dynamics. A time-depth perspective is crucially im-
350 portant in order to model the relationship between individual behavioural mechanisms and group
351 behavioural dynamics (Biro et al., 2016).

352 The Internet-based experimentation allowed us to conduct a real-time interactive behavioural
353 task with larger subject pools than a conventional laboratory-based experiment. This enabled us
354 not only to quantify the individual-level learning-and-decision processes (e.g. Ahn et al., 2014;
355 Daw et al., 2006) but also to map these individual-level processes on to the larger-scale collec-
356 tive behaviour (Raafat et al., 2009; Salganik et al., 2006; Sumpter, 2010). Although there are
357 always questions about the validity of participants' behaviour when deploying the web-based
358 method, we believe that the computational modelling approach coupled with higher statistical

359 power due to the large sample size, compensates for any drawbacks. The fact that our learning
360 model could approximate the participants' decision trajectories effectively suggest that most of
361 the participants engaged seriously with solving the task. An increasing body of evidence sup-
362 ports the argument that web-based behavioural experiments are as reliable as results from the
363 laboratory (e.g. Dandurand et al., 2008; Hergueux and Jacquemet, 2015).

364 The diverse effects of social influence on the collective wisdom of a group has been drawing
365 substantial attention (e.g. Becker et al., 2017; Jayles et al., 2017; Lorenz et al., 2011; Lorge et al.,
366 1958; Muchnik et al., 2013). The bulk of this literature, including many jury models and elec-
367 tion models (Hastie and Kameda, 2005; List, 2004), has focused primarily on the static estimation
368 problem, where the 'truth' is fixed from the outset. However, in reality, there are many situations
369 under which the state of the true value is changing over time so that monitoring and tracking
370 the pattern of change is a crucial determinant of decision performance (Payzan-Lenestour and
371 Bossaerts, 2011). In such temporally dynamic environments, decision-making and learning are
372 coordinated to affect future behavioural outcomes recursively (Sutton and Barto, 1998). Our
373 experimental task provides a simple vehicle for exploring collective intelligence in a dynamic
374 situation, which encompasses this learning-and-decision-making feedback loop. Potentially, in-
375 tegrating the wisdom of crowds with social learning and collective dynamics research will facil-
376 itate the more tractable use of swarm intelligence in a temporary changing world.

377 4 Material and methods

378 4.1 Computational learning-and-decision model

379 We modelled a learning and decision process based on standard reinforcement-learning theory
380 (Sutton and Barto, 1998). Following previous empirical studies of social learning strategies in
381 humans (e.g. McElreath et al., 2005, 2008; Toyokawa et al., 2017), our model consists of two
382 steps. First, an individual i updates the estimated average reward associated with an option m at
383 round t , namely Q-value ($Q_{i,t}(m)$), according to the Rescorla-Wagner rule (Trimmer et al., 2012)
384 as follows:

$$Q_{i,t+1}(m) = Q_{i,t}(m) + \alpha_i \mathbb{1}(m, m_{i,t}) (r_{i,t}(m) - Q_{i,t}(m)), \quad (3)$$

385 where α_i ($0 \leq \alpha_i \leq 1$) is a *learning rate* parameter of individual i determining the weight given to
386 new experience and $r_{i,t}(m)$ is the amount of monetary reward obtained from choosing the option
387 m in round t . $\mathbb{1}(m, m_{i,t})$ is the binary action-indicator function of individual i , given by

$$\mathbb{1}(m, m_{i,t}) = \begin{cases} 1, & \text{if } m_{i,t} = m \text{ or } t = 1, \\ 0, & \text{otherwise.} \end{cases} \quad (4)$$

388 Therefore, $Q_{i,t}(m)$ is updated only when the option m was chosen; when the option m was not
389 chosen, $Q_{i,t}(m)$ is not updated (i.e. $Q_{i,t+1}(m) = Q_{i,t}(m)$). Note that, only in the first round $t = 1$,
390 all Q-values are updated by using the chosen option's reward $r_{i,1}(m)$, so that the individual can
391 set a naive 'intuition' about the magnitude of reward values she/he would expect to earn from a
392 choice in the task; namely, $Q_{i,t=2}(1) = Q_{i,t=2}(2) = Q_{i,t=2}(3) = \alpha_i r_{i,t=1}(m)$. In practical terms,

393 this prevents the model from being overly sensitive to the first experience. Before the first choice,
394 individuals had no prior preference for either option (i.e. $Q_{i,1}(1) = Q_{i,1}(2) = Q_{i,1}(3) = 0$).

395 Second, a choice is made for an option m by individual i at the choice probability $P_{i,t}(m)$ that
396 is determined by a weighted average of social and asocial influences:

$$P_{i,t}(m) = \sigma_{i,t} S_{i,t}(m) + (1 - \sigma_{i,t}) A_{i,t}(m), \quad (5)$$

397 where $\sigma_{i,t}$ is the *social learning weight* ($0 \leq \sigma_{i,t} \leq 1$), and $S_{i,t}(m)$ and $A_{i,t}(m)$ are social and
398 asocial influences on the choice probability, respectively ($0 \leq S_{i,t}(m) \leq 1$ and $0 \leq A_{i,t}(m) \leq 1$).

399 Note that the sum of choice probabilities, the sum of social influences and the sum of asocial
400 influences are all equal to 1; namely, $\sum_{k \in \text{options}} P_{i,t}(k) = 1$, $\sum_k S_{i,t}(k) = 1$ and $\sum_k A_{i,t}(k) = 1$.

401 As for the asocial influence $A_{i,t}$, we assumed the so-called softmax (or logit choice) function,
402 which is widely used in the reinforcement-learning literature:

$$A_{i,t}(m) = \frac{\exp(\beta_{i,t} Q_{i,t}(m))}{\sum_{k \in \text{options}} \exp(\beta_{i,t} Q_{i,t}(k))}, \quad (6)$$

403 where $\beta_{i,t}$, called *inverse temperature*, manipulates individual i 's sensitivity to the Q-values (in
404 other words, controlling the proneness to explore). As $\beta_{i,t}$ goes to zero, asocial influence approx-
405 imates to a random choice (i.e. highly explorative). Conversely, if $\beta_{i,t} \rightarrow +\infty$, the asocial influ-
406 ence leads to a deterministic choice in favour of the option with the highest Q-value (i.e. highly
407 exploitative). For intermediate values of $\beta_{i,t}$, individual i exhibits a balance between exploration
408 and exploitation (Daw et al., 2006; Toyokawa et al., 2017). We allowed for the possibility that
409 the balance between exploration-exploitation could change as the task proceeds. To depict such
410 time dependence in exploration, we used the equation: $\beta_{i,t} = \beta_{i,0}^* + \epsilon_i t / 70$. If the slope ϵ_i is

411 positive (negative), asocial influence $A_{i,t}$ becomes more and more exploitative (explorative) as
412 round t increases. For a model fitting purpose, the time-dependent term $\epsilon_i t$ is scaled by the total
413 round number 70.

414 We modelled the social influence (i.e. the frequency-dependent copying) on the probability
415 that individual i chooses option m at round t as follows (McElreath et al., 2005, 2008; Aplin et al.,
416 2017; Barrett et al., 2017):

$$S_{i,t}(m) = \frac{\left(F_{t-1}(m) + 0.1\right)^{\theta_i}}{\sum_{k \in \text{options}} \left(F_{t-1}(k) + 0.1\right)^{\theta_i}}, \quad (7)$$

417 where $F_{t-1}(m)$ is a number of choices made by other individuals (excluding her/his own choice)
418 for the option m in the preceding round $t - 1$ ($t \geq 2$). θ_i is individual i 's *conformity exponent*,
419 $-\infty \leq \theta_i \leq +\infty$. When this exponent is larger than zero, higher social influence is given to
420 an option which was chosen by more individuals (i.e. positive frequency bias). When $\theta_i < 0$,
421 on the other hand, higher social influence is given to an option that fewer individuals chose in
422 the preceding round $t - 1$ (i.e. negative frequency bias). To implement the negative frequency
423 dependence, we added a small number 0.1 to F so that an option chosen by no one (i.e. $F_{t-1} = 0$)
424 could provide the highest social influence when $\theta_i < 0$. Note, there is no social influence when
425 $\theta_i = 0$ because in this case the 'social influence' favours a uniformly random choice, $S_{i,t}(m) =$
426 $1/(1 + 1 + 1) = 1/3$, independent of the social frequency distribution. Note also that, in the
427 first round $t = 1$, we assumed that the choice is only determined by the asocial softmax function
428 because there is no social information available.

429 We considered that the social learning weight $\sigma_{i,t}$ could change over time as assumed in the
430 inverse temperature $\beta_{i,t}$. To let $\sigma_{i,t}$ satisfy the constraint $0 \leq \sigma_{i,t} \leq 1$, we used the following

431 sigmoidal function:

$$\sigma_{i,t} = \frac{1}{1 + \exp(-(\sigma_{i,0}^* + \delta_i t/70))}. \quad (8)$$

432 If the slope δ_i is positive (negative), the social influence increases (decreases) over time. We
433 set the social learning weight equal to zero when group size is one (i.e. when an individual
434 participated in the task alone and/or when $\sum_{k \in \text{options}} F_{t-1}(k) = 0$).

435 We modelled both the inverse temperature $\beta_{i,t}$ and the social learning weight $\sigma_{i,t}$ as a time
436 function since otherwise it would be challenging to distinguish different patterns of learning in
437 this social learning task (Barrett, 2018). The parameter recovery test confirmed that we were
438 able to differentiate such processes under these assumptions (Figure S8-S12). While we also
439 considered the possibility of the conformity exponent being time-dependent (i.e. $\theta_{i,t} = \theta_{i,0}^* +$
440 $\gamma_i t/70$), the parameter recovery test suggested that the individual slope parameter γ_i was not
441 reliably recovered (Figure S20 and S21), and hence we concentrated our analysis on the time-
442 independent θ_i model. We confirmed that instead using the alternative model where both social
443 learning parameters were time-dependent (i.e. $\sigma_{i,t}$ and $\theta_{i,t}$) did not qualitatively change our results
444 (Figure S25 and S26).

445 In summary, the model has six free parameters that were estimated for each individual human
446 participant; namely, α_i , $\beta_{i,0}^*$, ϵ_i , $\sigma_{i,0}^*$, δ_i , and θ_i . To fit the model, we used a hierarchical Bayesian
447 method (HBM), estimating the global means (μ_α , $\mu_{\beta_0^*}$, μ_ϵ , $\mu_{\sigma_0^*}$, μ_δ , and μ_θ) and the global vari-
448 ations (ν_α , $\nu_{\beta_0^*}$, ν_ϵ , $\nu_{\sigma_0^*}$, ν_δ , and ν_θ) for each of the three experimental conditions (i.e. the Low-,
449 Moderate- and High-uncertain condition), which govern overall distributions of individual pa-
450 rameter values. It has become recognised that the HBM can provide more robust and reliable

451 parameter estimation than conventional maximum likelihood point estimation in complex cogni-
452 tive models (e.g. Ahn et al., 2014), a conclusion with which our parameter recovery test agreed
453 (Figure S10-S12).

454 **4.2 Agent-based model simulation**

455 We ran a series of individual-based model simulations assuming that a group of individuals play
456 our three-armed bandit task (under the Moderate-uncertainty condition) and that individuals be-
457 have in accordance with the computational learning-and-decision model. We varied the group
458 size ($n \in \{3, 10, 30\}$), the mean social learning weight ($\bar{\sigma} \in \{0.01, 0.1, 0.2, 0.3, \dots, 0.9\}$) and
459 the mean conformity exponent ($\bar{\theta} \in \{0.5, 1, 3, 6\}$), running 10,000 replications for each of the
460 possible parameter \times group size combinations. As for the other parameter values (e.g. the aso-
461 cial reinforcement learning parameters; $\alpha, \beta_0^*, \epsilon$), here we used the experimentally fitted global
462 means (Table 2 and Table S1). Relaxation of this assumption (i.e. using a different set of aso-
463 cial learning parameters) does not qualitatively change our story (e.g. Figure S4-S7). Note that
464 each individual's parameter values were randomly drawn from the distributions centred by the
465 global mean parameter values fixed to each simulation run. Therefore, the actual composition
466 of individual parameter values were different between individuals even within the same social
467 group.

468 **4.3 Participants in the online experiment**

469 A total of 755 subjects (354 females, 377 males, 2 others and 22 unspecified; mean age (1 *s.d.*) =
470 34.33 (10.9)) participated in our incentivised economic behavioural experiment (Figure S2). The

471 experimental sessions were conducted in December 2015 and in January 2016. We excluded
472 subjects who disconnected to the online task before completing at least the first 30 rounds from
473 our learning model fitting analysis, resulted in 699 subjects (573 subjects entered the group (i.e.
474 $n \geq 2$) condition and 126 entered the solitary (i.e. $n = 1$) condition). The task was advertised
475 using Amazon's Mechanical Turk (AMT; <https://www.mturk.com>; see Video S1; Video S2),
476 so that the participants could enter anonymously through their own internet browser window.
477 Upon connecting to the experimental game web page, the participants might be required to wait
478 on other participants at the virtual 'waiting room' for up to 5 minutes or until the requisite number
479 of participants arrived, whichever was sooner, before the task starts. The participants were payed
480 25 cents for a show-up fee plus a waiting-bonus at a rate of 12 cents per minute (i.e. *pro rata*
481 to 7.2 USD per hour) and a game bonus ($mean \pm 1s.d. = 1.7 \pm 0.79$ USD) depending on their
482 performance in the task. The total time, including net time spent in the waiting room, tended to
483 be less than 10 minutes.

484 **4.4 The online three-armed bandit task**

485 The participants performed a three-armed bandit task for 70 rounds. Each round started with the
486 choice stage at which three slot machines appeared on the screen (Figure S1; Video 1). Partic-
487 ipants chose a slot by clicking the mouse pointer (or tapping it if they used a tablet computer).
488 Participants had a maximum of 8 seconds to make their choices. If no choice was made during
489 the choice stage, a 'TIME OUT' message appeared in the centre of the screen without a monetary
490 reward (average number of missed rounds per participant was 0.18 out of 70 rounds). Partici-
491 pants were able to know the rest of the choice time by seeing a 'count-down bar' shown at the

492 top of the experimental screen.

493 Each option yielded monetary rewards randomly drawn from a normal probability distribu-
494 tion unique to each slot, rounded up to the next integer, or truncated to zero if it would have been a
495 negative value (Figure S3). The standard deviations of the probabilistic payoff distributions were
496 identical for all slots and did not change during the task (the *s.d.* = 0.55; although it actually was
497 slightly smaller than 0.55 due to the zero-truncation). The mean values of the probabilistic pay-
498 off were different between the options. ‘Poor’, ‘good’ and ‘excellent’ slots generated the lowest,
499 intermediate and the highest rewards on average, respectively. In the first 40 rounds, there were
500 two poor and one good options. After the round 40th, one of the poor option abruptly changed to
501 an excellent option (i.e. environmental change), and from the 41st round there were poor, good
502 and excellent options.

503 Once all the participants in the group made a choice (or had been time-outed), they proceeded
504 to the feedback stage in which they could see their own payoff from the current choice for two
505 seconds (‘0’ was shown if they had been time-outed), while they could not see others’ reward
506 values. After this feedback stage, subjects proceeded to the next round’s choice stage. From the
507 second round, a distribution of choices made by all participants in the group at the preceding
508 round (i.e. the social frequency information) was shown below each slot.

509 Before the task started, participants had read an illustrated instruction which told them that
510 they would play 70 rounds of the task, that the payoff would be randomly generated per choice
511 but associated with a probability distribution unique to each slot machine, i.e. the profitability
512 of the slot might be different from each other, that the environment might change during the
513 task so that the mean payoff from the slots might secretly change during the task, and that their

514 total payout were decided based on the sum of all earnings they achieved in the task. We also
515 explicitly informed subjects that all participants in the same group played the identical task so
516 that they could infer that the social information was informative. However, we did not specify
517 either the true mean payoff values associated with each option, or when and how the mean payoff
518 would actually change. After reading these instructions, participants proceeded to a ‘tutorial task’
519 without any monetary reward and without the social frequency information, so as to become
520 familiar with the task.

521 After they completed the behavioural task or were excluded from the task due to a bad internet
522 connection or due to opening another browser window during the task (see the ‘Reducing the risk
523 of cheating’ section in the appendix), subjects proceeded to a brief questionnaire page asking
524 about demographic information, which were skippable. Finally, the result screen was shown,
525 informing the total monetary reward she/he earned as well as a confirmation code unique for each
526 participant. Participants could get monetary reward through AMT by inputting the confirmation
527 code into the form at the AMT’s task page.

528 **4.5 Manipulating the group size and uncertainty**

529 To manipulate the size of each group, we varied the capacity of the waiting room from 10 to 30.
530 Because the task was being advertised on the Worker website at AMT for approximately 2 hours,
531 some participants occasionally arrived after the earlier groups had already started. In that case
532 the participant entered the newly opened waiting room which was open for the next 5 minutes.
533 The number of participants arriving declined with time because newly posted alternative tasks
534 were advertised on the top of the task list, which decreased our task’s visibility. This meant that

535 a later-starting session tended to begin before reaching maximum room capacity, resulting in the
536 smaller group size. Therefore, the actual size differed between groups.

537 To investigate the effect of the task uncertainty, we manipulated the closeness of each option's
538 mean payoff value, setting three different conditions in a between-group design. The three condi-
539 tions were: Low-uncertainty condition (differences between mean payoffs were 1.264; $N = 113$),
540 Moderate-uncertainty condition (differences between mean payoffs were 0.742; $N = 132$) and
541 High-uncertainty condition (differences between mean payoffs were 0.3; $N = 454$). The mean
542 payoff associated with the 'excellent' slot in all three conditions was fixed to 3.1 cents (Figure
543 S3). These conditions were randomly assigned for each experimental session. However, we re-
544 cruited more participants in the High-uncertainty condition compared to the other two because
545 we expected that larger group sizes would be needed to generate the collective wisdom in noisier
546 environments.

547 **4.6 Statistical analysis**

548 We used a hierarchical Bayesian method (HBM) to estimate the free parameters of our statis-
549 tical models, including the computational learning-and-decision-making model. The HBM al-
550 lows us to estimate individual differences, while ensures these individual variations are bounded
551 by the group-level global parameters. The HBM was performed under Stan 2.16.2 ([http:](http://mc-stan.org)
552 [//mc-stan.org](http://mc-stan.org)) in R 3.4.1 (<https://www.r-project.org>) software. The models contained
553 at least 4 parallel chains and we confirmed convergence of the MCMC using both the Gelman-
554 Rubin statistics and the effective sample sizes. Full details of the model fitting procedure and
555 prior assumptions are shown in the appendix.

556 **4.6.1 Parameter recovery test**

557 To check the validity of our model-fitting method, we conducted a ‘parameter recovery test’
558 so as to examine how well our model fitting procedure had been able to reveal true individual
559 parameter values. To do this, we generated synthetic data by running a simulation with the
560 empirically fitted global parameter values, and then re-fitted the model with this synthetic data
561 using the same procedure. The parameter recovery test showed that the all true global parameter
562 values were fallen into the 95% Bayesian credible interval (Figure S8), and at least 93% of the
563 true individual parameter values were correctly recovered (i.e. 96% of α_i , 93% of $\beta_{i,0}^*$, 95% of
564 ϵ_i , 97% of $\sigma_{i,0}^*$, 96% of δ_i and 97% of θ_i values were fallen into the 95% Bayesian CI. Figure
565 S9-S12).

566 **4.6.2 Categorisation of individual learning strategies**

567 Based on the 50% CI of the individual *conformity exponent* parameter values θ_i , we divided
568 the participants into the following three different social learning strategies. If her/his 50% CI
569 of θ_i fell above zero ($\theta_{lower} > 0$), below zero ($\theta_{upper} < 0$) or including zero ($\theta_{lower} \leq 0 \leq$
570 θ_{upper}), she/he was categorised as a ‘positive frequency-dependent copier’, a ‘negative frequency-
571 dependent copier’, or a ‘random choice individual’, respectively. We used the 50% Bayesian CI
572 to conduct this categorisation instead of using the more conservative 95% CI because the latter
573 would cause much higher rates of ‘false negatives’, by which an individual who applied either a
574 positive frequency-dependent copying or a negative-frequency dependent copying strategy was
575 falsely labelled as an asocial random choice individual (Figure S10d). Four hundred agents out
576 of 572 ($\approx 70\%$) were falsely categorised as a random choice learner in the recovery test when we

577 used the 95% criterion (Figure S10d). On the other hand, the 50% CI criterion seemed to be much
578 better in terms of the false negative rate which was only 18.5% (i.e. 106 agents), although it might
579 be slightly worse in terms of ‘false positives’: Thirty-seven agents (6.5%) were falsely labelled
580 as either a positive frequency-dependent copier or a negative-frequency dependent copier by the
581 50% CI, whereas the false positive rate of the 95% CI was only 0.2% (Figure S10e). To balance
582 the risk of false positives and false negatives, we decided to use the 50% CI which seemed to
583 have more strategy detecting power.

584 **4.6.3 Generalised linear mixed models**

585 To examine whether increasing group size and increasing task uncertainty affected individual
586 use of the positive frequency-dependent copying strategy, we used a hierarchical Bayesian logis-
587 tic regression model with a random effect of groups. The dependent variable was whether the
588 participant used the positive frequency-dependent copying (1) or not (0). The model includes
589 fixed effects of group size (standardised), task uncertainty (0: Low, 0.5: Moderate, 1: High), age
590 (standardised), gender (0: male, 1: female, NA: others or unspecified), and possible two-way
591 interactions between these fixed effects.

592 We also investigated the effects of both group size and the task’s uncertainty on the fitted
593 values of the learning parameters. We used a hierarchical Bayesian gaussian regression model
594 predicting the individual fitted parameter values. The model includes effects of group size (stan-
595 dardised), task uncertainty (0: Low, 0.5: Moderate, 1: High), age (standardised), gender (0:
596 male, 1: female, NA: others or unspecified), and two-way interactions between these fixed ef-
597 fects. We assumed that the variance of the individual parameter values might be contingent upon

598 task uncertainty because we had found in the computational model-fitting result that the fitted
599 global variance parameters (i.e. $v_{\sigma_0^*}$, v_δ and v_θ) were larger in more uncertain conditions (Table
600 S1).

601 **4.6.4 Post-hoc model simulation for Figure 4d-f**

602 So as to evaluate how accurately our model can generate observed decision pattern in our task
603 setting, we ran a series of individual-based model simulation using the fitted individual param-
604 eter values (i.e. means of the individual posterior distributions) for each group size for each
605 uncertainty condition. At the first step of the simulation, we assigned a set of fitted parameters
606 of a randomly-chosen experimental subject from the same group size and the same uncertain
607 condition to an simulated agent, until the number of agents reaches the simulated group size. We
608 allowed duplicate choice of experimental subject in this parameter assignment. At the second
609 step, we let this synthetic group of agents play the bandit task. We repeated these steps 5,000
610 times for each group size, task uncertainty.

611 **4.7 Code and data availability**

612 The browser based online task was built by Node.js (<https://nodejs.org/en/>) and socket.io
613 (<https://socket.io>), and the code are available on a GitHub repository ([https://github.
614 com/WataruToyokawa/MultiPlayerThreeArmedBanditGame](https://github.com/WataruToyokawa/MultiPlayerThreeArmedBanditGame)). Analyses were conducted in
615 R (<https://www.r-project.org>) and simulations of individual based models were conducted
616 in Mathematica (<https://www.wolfram.com>), both of which including data are available on
617 an online repository ([URL will appear after acceptance from a journal](#)).

618 **5 Ethics statement**

619 This study was approved by University of St Andrews (BL10808).

620 **6 Competing interest**

621 We have no competing interest.

622 **7 Authors' contributions**

623 WT, AW and KNL planned the study and built the computational model. WT ran simulations.

624 WT and AW made the experimental material, ran the web-base experiment, and collected the

625 experimental data. WT, AW and KNL analysed the data and wrote the manuscript.

626 **8 Acknowledgements**

627 **9 Funding**

628 This research was supported by The John Templeton Foundation (KNL; 40128) and Suntory

629 Foundation Research Support (WT; 2015-311). WT was supported by JSPS Overseas Research

630 Fellowships (H27-11).

631 **References**

632 Ahn, W. Y., Vasilev, G., Lee, S. H., Busemeyer, J. R., Kruschke, J. K., Bechara, A., and Vassileva,
633 J. (2014). Decision-making in stimulant and opiate addicts in protracted abstinence: Evidence
634 from computational modeling with pure users. *Frontiers in Psychology*, 5(AUG):1–15. (doi:
635 10.3389/fpsyg.2014.00849.

636 Aplin, L. M., Sheldon, B. C., and McElreath, R. (2017). Conformity does not perpetuate sub-
637 optimal traditions in a wild population of songbirds. *Proceedings of the National Academy of*
638 *Sciences*, page 201621067. (doi: 10.1073/PNAS.1621067114.

639 Arbilly, M., Motro, U., Feldman, M. W., and Lotem, A. (2011). Evolution of social learning when
640 high expected payoffs are associated with high risk of failure. *Journal of the Royal Society,*
641 *Interface / the Royal Society*, 8(64):1604–15. (doi: 10.1098/rsif.2011.0138.

642 Barrett, B. J. (2018). Equifinality in empirical studies of cultural transmission. *Behavioural*
643 *Processes*. (doi: 10.1016/j.beproc.2018.01.011.

644 Barrett, B. J., Mcelreath, R. L., Perry, S. E., and Barrett, B. J. (2017). Pay-off-biased social
645 learning underlies the diffusion of novel extractive foraging traditions in a wild primate. *Pro-*
646 *ceedings of Royal Society B*, 284.

647 Becker, J., Brackbill, D., and Centola, D. (2017). Network dynamics of social influence in the
648 wisdom of crowds. *Proceedings of the National Academy of Sciences*, page 201615978. (doi:
649 10.1073/pnas.1615978114.

650 Berdahl, A., Torney, C., Ioannou, C., Faria, J., and Couzin, I. (2013). Emergent Sensing of

- 651 Complex Environments by Mobile Animal Groups. *Science*, 339:574–576. (doi: 10.1126/sci-
652 ence.1229262.
- 653 Bikhchandani, S., Hirshleifer, D., and Welch, I. (1992). A Theory of Fads, Fashion, Custom, and
654 Cultural Change as Informational Cascades. *Journal of Political Economy*, 100(5):992. (doi:
655 10.1086/261849.
- 656 Biro, D., Sasaki, T., and Portugal, S. J. (2016). Bringing a Time-Depth Perspective to
657 Collective Animal Behaviour. *Trends in Ecology and Evolution*, 31(7):550–562. (doi:
658 10.1016/j.tree.2016.03.018.
- 659 Bonabeau, E., Dorigo, M., and Theraulaz, G. (1999). *Swarm Intelligence: From Natural to*
660 *Artificial Systems*. Oxford University Press, New York, NY.
- 661 Bond, R. (2005). Group Size and Conformity. *Group Processes & Intergroup Relations*,
662 8(4):331–354. (doi: 10.1177/1368430205056464.
- 663 Boyd, R. and Richerson, P. J. (1985). *Culture and the Evolutionary Process*. University of
664 Chicago Press, Chicago, IL.
- 665 Boyd, R. and Richerson, P. J. (1989). Social learning as an adaptation. *Lectures on Mathematics*
666 *in the Life Sciences*, 20:1–26.
- 667 Camazine, S., Deneubourg, J.-L., Franks, N. R., Sneyd, J., Theraulaz, G., and Bonabeau, E.
668 (2001). *Self-Organization in Biological Systems*. Princeton University Press, Princeton, NJ.
- 669 Chari, V. V. and Kehoe, P. J. (2004). Financial crises as herds: Overturning the critiques. *Journal*
670 *of Economic Theory*, 119(1 SPEC. ISS.):128–150. (doi: 10.1016/S0022-0531(03)00225-4.

- 671 Cronin, A. L. (2016). Group size advantages to decision making are environmentally
672 contingent in house-hunting Myrmecina ants. *Animal Behaviour*, 118:171–179. (doi:
673 10.1016/j.anbehav.2016.06.010.
- 674 Dandurand, F., ShultzEmail, T. R., and Onishi, K. H. (2008). Comparing online and lab meth-
675 ods in a problem-solving experiment. *Behavior Research Methods*, 40(2):428–434. (doi:
676 10.3758/BRM.40.2.428.
- 677 Daw, N. D., O’Doherty, J. P., Dayan, P., Seymour, B., and Dolan, R. J. (2006). Cortical substrates
678 for exploratory decisions in humans. *Nature*, 441(7095):876–9. (doi: 10.1038/nature04766.
- 679 Dingemanse, N. J., Kazem, A. J., Réale, D., and Wright, J. (2010). Behavioural reaction norms:
680 animal personality meets individual plasticity. *Trends in Ecology and Evolution*, 25(2):81–89.
681 (doi: 10.1016/j.tree.2009.07.013.
- 682 Efferson, C., Lalive, R., Richerson, P. J., McElreath, R., and Lubell, M. (2008). Conformists and
683 mavericks: the empirics of frequency-dependent cultural transmission. *Evolution and Human
684 Behavior*, 29:56–64. (doi: 10.1016/j.evolhumbehav.2007.08.003.
- 685 Feldman, M. W., Aoki, K., and Kumm, J. (1996). Individual Versus Social Learning: Evolution-
686 ary Analysis in a Fluctuating Environment. *Anthropological Science*, 104(3):209–231. (doi:
687 10.1537/ase.104.209.
- 688 Franks, N. R., Mallon, E. B., Bray, H. E., Hamilton, M. J., and Mischler, T. C. (2003). Strategies
689 for choosing between alternatives with different attributes: exemplified by house-hunting ants.
690 *Animal Behaviour*, 65(1):215–223. (doi: 10.1006/anbe.2002.2032.

- 691 Giraldeau, L.-A., Valone, T. J., and Templeton, J. J. (2002). Potential disadvantages of using
692 socially acquired information. *Philosophical transactions of the Royal Society of London.
693 Series B, Biological sciences*, 357(1427):1559–66. (doi: 10.1098/rstb.2002.1065.
- 694 Gray, J., Hilton, J., and Bijak, J. (2017). Choosing the choice: Reflections on modelling deci-
695 sions and behaviour in demographic agent-based models. *Population Studies*, 71:85–97. (doi:
696 10.1080/00324728.2017.1350280.
- 697 Hastie, R. and Kameda, T. (2005). The robust beauty of majority rules in group decisions.
698 *Psychological review*, 112(2):494–508. (doi: 10.1037/0033-295X.112.2.494.
- 699 Hergueux, J. and Jacquemet, N. (2015). Social preferences in the online laboratory: a randomized
700 experiment. *Experimental Economics*, 18(2):251–283. (doi: 10.1007/s10683-014-9400-5.
- 701 Hoppitt, W. and Laland, K. N. (2013). *Social Learning: An Introduction to Mechanisms, Meth-
702 ods, and Models*. Princeton University Press.
- 703 Janis, I. L. (1972). *Victims of groupthink: A psychological study of foreign policy*. Houghton
704 Mifflin Company, Boston, NY.
- 705 Jayles, B., Kim, H.-r., Escobedo, R., Cezera, S., Blanchet, A., Kameda, T., Sire, C., and
706 Theraulaz, G. (2017). How social information can improve estimation accuracy in hu-
707 man groups. *Proceedings of the National Academy of Sciences*, 114(47):201703695. (doi:
708 10.1073/pnas.1703695114.
- 709 Jolles, J. W., Laskowski, K. L., Boogert, N. J., and Manica, A. (2018). Repeatable group differ-

710 ences in the collective behaviour of stickleback shoals across ecological contexts. *Proceedings*
711 *of Royal Society B*, pages 13–16.

712 Kameda, T. and Hastie, R. (2015). Herd Behavior. In *Emerging Trends in the Social and Behav-*
713 *ioral Sciences: An Interdisciplinary, Searchable, and Linkable Resource*, pages 1–14. Wiley
714 Online Library.

715 Kameda, T. and Nakanishi, D. (2002). Cost–benefit analysis of social/cultural learning in a
716 nonstationary uncertain environment. *Evolution and Human Behavior*, 23(5):373–393. (doi:
717 10.1016/S1090-5138(02)00101-0.

718 Kandler, A. and Laland, K. N. (2013). Tradeoffs between the strength of conformity and number
719 of conformists in variable environments. *Journal of theoretical biology*, 332:191–202. (doi:
720 10.1016/j.jtbi.2013.04.023.

721 Kendal, R. L., Coolen, I., and Laland, K. N. (2004). The role of conformity in foraging when per-
722 sonal and social information conflict. *Behavioral Ecology*, 15(2):269–277. (doi: 10.1093/be-
723 heco/arh008.

724 King, A. J. and Cowlshaw, G. (2007). When to use social information: the advantage
725 of large group size in individual decision making. *Biology letters*, 3(2):137–139. (doi:
726 10.1098/rsbl.2007.0017.

727 King, A. J. and Sueur, C. (2011). Where Next? Group Coordination and Collective Deci-
728 sion Making by Primates. *International Journal of Primatology*, 32(6):1245–1267. (doi:
729 10.1007/s10764-011-9526-7.

- 730 Kline, M. A. and Boyd, R. (2010). Population size predicts technological complexity in Ocea-
731 nia. *Proceedings of the Royal Society B: Biological Sciences*, 277(1693):2559–2564. (doi:
732 10.1098/rspb.2010.0452.
- 733 Krause, J. and Ruxton, G. D. (2002). *Living in groups*. Oxford University Press, Oxford, New
734 York.
- 735 Krause, J., Ruxton, G. D., and Krause, S. (2010). Swarm intelligence in animals and humans.
736 *Trends in ecology & evolution*, 25(1):28–34. (doi: 10.1016/j.tree.2009.06.016.
- 737 Krause, S., James, R., Faria, J. J., Ruxton, G. D., and Krause, J. (2011). Swarm intelli-
738 gence in humans: diversity can trump ability. *Animal Behaviour*, 81(5):941–948. (doi:
739 10.1016/j.anbehav.2010.12.018.
- 740 Laan, A., Madirolas, G., and Polavieja, G. G. D. (2017). Rescuing collective wisdom when
741 the average group opinion is wrong. *Frontiers in Robotics and AI*, 4(November):1–28. (doi:
742 10.3389/frobt.2017.00056.
- 743 Laland, K. N. (2004). Social learning strategies. *Animal Learning & Behavior*, 32(1):4–14. (doi:
744 10.3758/BF03196002.
- 745 Le Bon, G. (1896). *The crowd: study of the popular mind*. Unwin, London, UK, 4th edition.
- 746 Liker, A. and Bokony, V. (2009). Larger groups are more successful in innovative problem
747 solving in house sparrows. *Proceedings of the National Academy of Sciences*, 106(19):7893–
748 7898. (doi: 10.1073/pnas.0900042106.

749 List, C. (2004). Democracy in animal groups: a political science perspective. *Trends in Ecology*
750 *and Evolution*, 19(4):166–168. (doi: 10.1016/j.tree.2004.02.001).

751 List, C., Elsholtz, C., and Seeley, T. D. (2009). Independence and interdependence in collective
752 decision making: an agent-based model of nest-site choice by honeybee swarms. *Philosophi-*
753 *cal transactions of the Royal Society of London. Series B, Biological sciences*, 364(1518):755–
754 762. (doi: 10.1098/rstb.2008.0277).

755 Lorenz, J., Rauhut, H., Schweitzer, F., and Helbing, D. (2011). How social influence can un-
756 dermine the wisdom of crowd effect. *Proceedings of the National Academy of Sciences of the*
757 *United States of America*, 108(22):9020–5. (doi: 10.1073/pnas.1008636108).

758 Lorge, I., Fox, D., Davitz, J., and Brenner, M. (1958). A survey of studies contrasting the qual-
759 ity of group performance and individual performance, 1920-1957. *Psychological Bulletin*,
760 55(6):337–372. (doi: 10.1037/h0042344).

761 Mackay, C. (1841). *Extraordinary Popular Delusions and the Madness of Crowds*. Richard
762 Bentley, London, UK.

763 McElreath, R., Bell, A. V., Efferson, C., Lubell, M., Richerson, P. J., and Waring, T. (2008).
764 Beyond existence and aiming outside the laboratory: estimating frequency-dependent and
765 pay-off-biased social learning strategies. *Philosophical transactions of the Royal Society of*
766 *London. Series B, Biological sciences*, 363(1509):3515–28. (doi: 10.1098/rstb.2008.0131).

767 McElreath, R., Lubell, M., Richerson, P. J., Waring, T. M., Baum, W., Edsten, E., Ef-
768 ferson, C., and Paciotti, B. (2005). Applying evolutionary models to the labora-

769 tory study of social learning. *Evolution and Human Behavior*, 26(6):483–508. (doi:
770 10.1016/j.evolhumbehav.2005.04.003.

771 Mesoudi, A. (2011). An experimental comparison of human social learning strategies: payoff-
772 biased social learning is adaptive but underused. *Evolution and Human Behavior*, 32(5):334–
773 342. (doi: 10.1016/j.evolhumbehav.2010.12.001.

774 Mesoudi, A., Chang, L., Dall, S. R., and Thornton, A. (2016). The Evolution of Individual
775 and Cultural Variation in Social Learning. *Trends in Ecology & Evolution*, xx:1–11. (doi:
776 10.1016/j.tree.2015.12.012.

777 Michelena, P., Jeanson, R., Deneubourg, J.-L., and Sibbald, A. M. (2010). Personality and col-
778 lective decision-making in foraging herbivores. *Proceedings. Biological sciences / The Royal*
779 *Society*, 277(1684):1093–9. (doi: 10.1098/rspb.2009.1926.

780 Morand-Ferron, J. and Quinn, J. L. (2011). Larger groups of passerines are more efficient prob-
781 lem solvers in the wild. *Proceedings of the National Academy of Sciences*, 108(38):15898–
782 15903. (doi: 10.1073/pnas.1111560108.

783 Morgan, T. J. H., Rendell, L. E., Ehn, M., Hoppitt, W., and Laland, K. N. (2012). The evolu-
784 tionary basis of human social learning. *Proceedings. Biological sciences / The Royal Society*,
785 279(1729):653–62. (doi: 10.1098/rspb.2011.1172.

786 Muchnik, L., Aral, S., and Taylor, S. J. (2013). Social influence bias: a randomized experiment.
787 *Science (New York, N.Y.)*, 341(6146):647–51. (doi: 10.1126/science.1240466.

- 788 Muthukrishna, M., Shulman, B. W., Vasilescu, V., and Henrich, J. (2014). Sociality influences
789 cultural complexity. *Proceedings of Royal Society B*, 281(November 2013):20132511.
- 790 Nicolis, S. and Deneubourg, J. (1999). Emerging patterns and food recruitment in ants: an
791 analytical study. *Journal of theoretical biology*, 198(4):575–92. (doi: 10.1006/jtbi.1999.0934.
- 792 Payzan-Lenestour, E. and Bossaerts, P. (2011). Risk, unexpected uncertainty, and estimation
793 uncertainty: Bayesian learning in unstable settings. *PLoS Computational Biology*, 7(1). (doi:
794 10.1371/journal.pcbi.1001048.
- 795 Planas-sitja, I., Deneubourg, J.-l., Gibon, C., and Sempo, G. (2015). Group personality during
796 collective decision-making : a multi-level approach. *Proceedings of the Royal Society B:
797 Biological Sciences*, 282:20142515.
- 798 Pratt, S. C. and Sumpter, D. J. T. (2006). A tunable algorithm for collective decision-making. *Pro-
799 ceedings of the National Academy of Sciences of the United States of America*, 103(43):15906–
800 10. (doi: 10.1073/pnas.0604801103.
- 801 Raafat, R. M., Chater, N., and Frith, C. (2009). Herding in humans. *Trends in cognitive sciences*,
802 13(10):420–8. (doi: 10.1016/j.tics.2009.08.002.
- 803 Reid, C. R. and Latty, T. (2016). Collective behaviour and swarm intelligence in slime moulds.
804 *FEMS Microbiology Reviews*, 40(6):798–806. (doi: 10.1093/femsre/fuw033.
- 805 Richerson, P. J. and Boyd, R. (2005). *Not By Genes Alone*. University of Chicago Press, Chicago,
806 IL.

- 807 Rosenberg, L. and Pescetelli, N. (2017). Amplifying Prediction Accuracy using Swarm A . I .
808 *Intelligent Systems Conference 2017*, (September):1–5.
- 809 Salganik, M. J., Dodds, P. S., and Watts, D. J. (2006). Experimental Study of Inequality and
810 Cultural Market. *Science*, 311(February).
- 811 Sasaki, T. and Biro, D. (2017). Cumulative culture can emerge from collective intelligence in
812 animal groups. *Nature Communications*, 8:1–6. (doi: 10.1038/ncomms15049).
- 813 Sasaki, T., Granovskiy, B., Mann, R. P., Sumpter, D. J. T., and Pratt, S. C. (2013). Ant
814 colonies outperform individuals when a sensory discrimination task is difficult but not when
815 it is easy. *Proceedings of the National Academy of Sciences*, 110(34):13769–13773. (doi:
816 10.1073/pnas.1304917110).
- 817 Sasaki, T. and Pratt, S. C. (2012). Groups have a larger cognitive capacity than individuals.
818 *Current biology : CB*, 22(19):R827–9. (doi: 10.1016/j.cub.2012.07.058).
- 819 Seeley, T., Camazine, S., and Sneyd, J. (1991). Collective decision-making in honey bees: how
820 colonies choose among nectar sources. *Behavioral Ecology and Sociobiology*, 28:277–290.
- 821 Seeley, T. D. and Visscher, P. K. (2004). Quorum sensing during nest-site selection by honeybee
822 swarms. *Behavioral Ecology and Sociobiology*, 56(6):594–601. (doi: 10.1007/s00265-004-
823 0814-5).
- 824 Shaffer, Z., Sasaki, T., and Pratt, S. C. (2013). Linear recruitment leads to allocation
825 and flexibility in collective foraging by ants. *Animal Behaviour*, 86(5):967–75. (doi:
826 10.1016/j.anbehav.2013.08.014).

- 827 Street, S. E., Navarrete, A. F., Reader, S. M., and Laland, K. N. (2017). Coevolution of cultural
828 intelligence , extended life history , sociality , and brain size in primates. *Proceedings of the*
829 *National Academy of Sciences*, 114(30):1–7. (doi: 10.1073/pnas.1620734114.
- 830 Sumpter, D. J. T. (2010). *Collective Animal Behavior*. Princeton University Press, Princeton,
831 NJ.
- 832 Sumpter, D. J. T., Krause, J., James, R., Couzin, I. D., and Ward, A. J. W. (2008). Consensus deci-
833 sion making by fish. *Current biology : CB*, 18(22):1773–7. (doi: 10.1016/j.cub.2008.09.064.
- 834 Sutton, R. S. and Barto, a. G. (1998). *Reinforcement learning: an introduction*. MIT Press,
835 Cambridge, MA. (doi: 10.1109/TNN.1998.712192.
- 836 Toyokawa, W., Kim, H.-R., and Kameda, T. (2014). Human Collective Intelligence under
837 Dual Exploration-Exploitation Dilemmas. *PloS one*, 9(4):e95789. (doi: 10.1371/jour-
838 nal.pone.0095789.
- 839 Toyokawa, W., Saito, Y., and Kameda, T. (2017). Individual differences in learning behaviours in
840 humans: asocial exploration tendency does not predict reliance on social learning. *Evolution*
841 *and Human Behavior*, 38(3):325–333. (doi: 10.1016/j.evolhumbehav.2016.11.001.
- 842 Trimmer, P. C., McNamara, J. M., Houston, A. I., and a.R. Marshall, J. (2012). Does natural
843 selection favour the Rescorla–Wagner rule? *Journal of Theoretical Biology*, 302:39–52. (doi:
844 10.1016/j.jtbi.2012.02.014.
- 845 Ward, A. J. W., Herbert-Read, J. E., Sumpter, D. J. T., and Krause, J. (2011). Fast and accurate

846 decisions through collective vigilance in fish shoals. *Proceedings of the National Academy of*
847 *Sciences*, 108(6):2312–2315. (doi: 10.1073/pnas.1007102108).

848 Webster, M. and Laland, K. (2008). Social learning strategies and predation risk: minnows copy
849 only when using private information would be costly. *Proceedings of the Royal Society B:*
850 *Biological Sciences*, 275(1653):2869–2876. (doi: 10.1098/rspb.2008.0817).

851 Webster, M. M. and Laland, K. N. (2011). Reproductive state affects reliance on public informa-
852 tion in sticklebacks. *Proceedings. Biological sciences / The Royal Society*, 278(1705):619–
853 627. (doi: 10.1098/rspb.2010.1562).

854 Webster, M. M., Whalen, A., and Laland, K. N. (2017). Fish pool their experience to solve
855 problems collectively. *Nature Ecology and Evolution*, 1(5):1–5. (doi: 10.1038/s41559-017-
856 0135).

857 Wolf, M., Kurvers, R. H. J. M., Ward, A. J. W., Krause, S., and Krause, J. (2013). Accurate
858 decisions in an uncertain world: collective cognition increases true positives while decreasing
859 false positives. *Proceedings. Biological sciences / The Royal Society*, 280(1756):20122777.
860 (doi: 10.1098/rspb.2012.2777).

1 **1 Appendix 1 Supplementary experimental procedure**

2 **1.1 Amazon Mechanical Turk**

3 The online task was advertised as a ‘HIT (Human Intelligence Task)’ entitled ‘Lottery Choice
4 Experiment (about 15 mins + fun + bonus!)’ in Amazon Mechanical Turk (AMT). The HIT was
5 only available for individuals whose ‘HIT Approval Rate’ was greater than or equal to 90% and
6 who live in the US.

7 On the advertisement page, we stressed that there could be extra payoff to subjects depending
8 on their performance in the task; that stability of their Internet connection was necessary; and
9 that they could participate in the task only once (Video S1).

10 At the bottom of the advertisement page, an URL link to our experimental server would
11 appear. The link was not shown until the participants decided to join the task. There were
12 also text forms into which the participants could input their own confirmation code, which they
13 would get by finishing the experimental task, and where they could add comments on the task.
14 By clicking the submit button below they could complete the task, allowing the monetary reward
15 to be paid through Amazon system.

16 **1.2 A written consent form and an instruction for the task**

17 On clicking the URL link shown at the bottom of the HIT advertisement page, participants pro-
18 ceeded to a consent form that emphasised data anonymity and asked them not to interact with
19 anyone during the task (Video S1). Scrolling this consent form page, participants proceeded to
20 sign the form. After answering all the YES/NO questions and inputting the CAPTCHA, partici-

21 pants could proceed to instructions.

22 On the first page of the instructions participants were informed that the study was split into
23 two parts: an interactive economic decision-making game and a short survey. On the second
24 page of the instructions the details of the decision task were explained with illustrations.

25 Full details and code of the task are available in GitHub ([https://github.com/WataruToyokawa/
26 MultiPlayerThreeArmedBanditGame](https://github.com/WataruToyokawa/MultiPlayerThreeArmedBanditGame)).

27 **1.3 Reducing the risk of cheating**

28 To minimise the risk of multiple accesses from the same person, we introduced the restriction
29 that a single ‘worker ID’ associated with participants’ AMT accounts, could participate only once
30 in the experiment. We rejected access from the same IP address: If a participant’s IP address had
31 already been stored in our database, the participant directly proceeded from the instruction page
32 to the questionnaire page. In that case, 25 cents show-up fee was still paid because it was possible
33 that different persons might use the same IP address.

34 To minimise the risk of opening other browser windows during the task (for example, brows-
35 ing other websites), we used ‘Page Visibility API’ ([https://developer.mozilla.org/en-US/
36 docs/Web/API/Page_Visibility_API](https://developer.mozilla.org/en-US/docs/Web/API/Page_Visibility_API)) to track whether the experimental browser window
37 was always active and not hidden by other browser windows or tabs for more than 1 second. If it
38 was detected that the experimental window was in a hidden state, the participant was automati-
39 cally redirected to the questionnaire page. In that case, 25 cents show-up fee plus a waiting-bonus
40 (if applicable) and a game-bonus earned so far were paid. In the instruction, participants were
41 warned not to open any other browser windows/tabs during the task and were informed that they

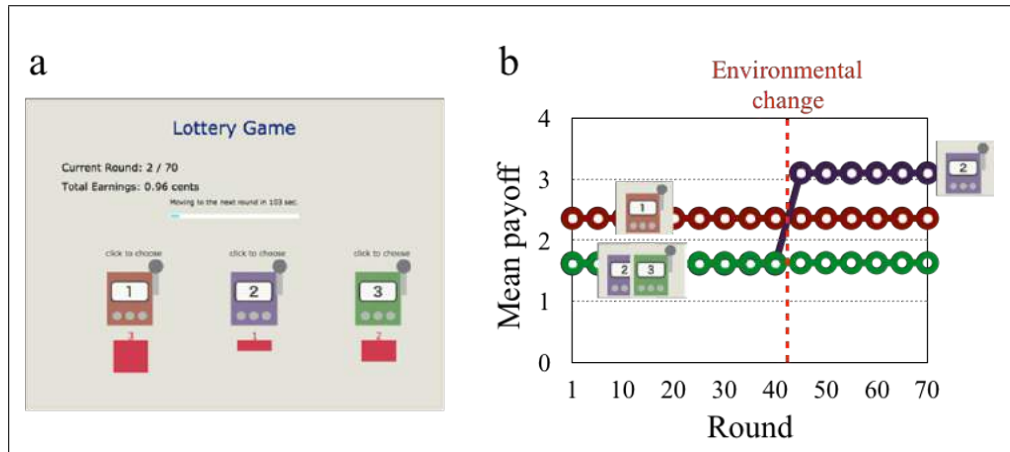


Figure S1. The three-armed bandit task. (a) Illustration of the user interface of the task. Participants could choose an option by clicking one of the slot machines. The frequency distribution of choices made by participants in the same group in the preceding round (i.e. the social frequency information) is shown by red numbers below each option. The lengths of the red bars are proportional to the social frequency distributions. Participants could also see their current total earnings (0.96 cents in this example) as well as the current round number (Round 2 in this example). (b) Example of mean payoffs for each option in the task. The payoff received for a particular choice is drawn from a Gaussian distribution with noise around each mean (with a fixed standard deviation: $1.S.D. = 0.55$). Note that the most profitable slot (the 'optimal option') was switched (i.e. environmental change) after 40 rounds: One 'poor' slot (slot-2 in this example) changed to an 'excellent' one at the beginning of the 41st round, while the other machines' expected returns were not changed. The association between each option's number and its payoff was randomly assigned across experimental sessions.

42 would be eliminated from the session if they did so.

43 **2 Appendix 2 Supplementary computational modelling procedure**

44 **2.1 Hierarchical Bayesian parameter estimation**

45 We used hierarchical Bayesian method (HBM) to estimate the free parameters of our learning
46 model. HBM allows us to estimate individual differences, while this individual variation is
47 bounded by the group-level (i.e. hyper) parameters. To perform HBM, we used Stan 2.16.2
48 in R 3.4.1.

49 In our model, there are 6 individual parameters; namely, α_i , $\beta_{i,0}^*$, ϵ_i , $\sigma_{i,0}^*$, δ_i , and θ_i . Because
50 the learning rate α_i is bounded between 0 and 1, we estimated α_i^* rather than α_i itself ($-\infty \leq$
51 $\alpha_i^* \leq +\infty$), which is given by the following sigmoidal function:

$$\alpha_i = \frac{1}{1 + \exp(-\alpha_i^*)}. \quad (1)$$

52 We assumed the Student's t distributions for individual random effects of each parameter so
53 as to allow a few 'outliers', because the Student's t distribution has a longer tail compared to a
54 normal distribution. To do so, we used the following reparameterization for each $parameter(.) \in$
55 $\{\alpha_i^*, \beta_{i,0}^*, \epsilon_i, \sigma_{i,0}^*, \delta_i, \theta_i\}$:

$$parameter(.)_i = \mu_{(.),c} + v_{(.),c} * parameter(.)_{raw}_i, \quad (2)$$

56 where $\mu_{(.),c}$ is a global mean of the $parameter(.)$ in the condition c ($c \in \{\text{Low-}, \text{Moderate-},$
57 $\text{High-uncertainty condition}\}$), and $v_{(.),c}$ is a global scale parameter of the individual variations in

58 condition c , which is multiplied by a standardised individual random variable $parameter(.)_{raw_i}$
59 drawn from

$$parameter(.)_{raw_i} \sim Student_t(df = 4, location = 0, scale = 1). \quad (3)$$

60 As for the global parameters, we used a normal and a half-normal prior distributions for $\mu_{(.),c}$
61 and $v_{(.),c}$, respectively:

$$\mu_{(.),c} \sim Normal(mean = 0, sd = 5), \quad (4a)$$

$$v_{(.),c} \sim Normal^+(mean = 0, sd = 3). \quad (4b)$$

62 In summary, there are 36 global free parameters (= 6 μ s and 6 v s for 3 different conditions
63 each). A total of 2000 iterations were performed after 1000 warm-up with thin = 5 for each of
64 8 chains (= 2000 samples / 5 steps \times 8 chains = a total of 3200 samples). We used the Gelman-
65 Rubin statistics (as known as \hat{R}) as well as the effective sample sizes (ESS) so as to check the
66 convergence of the MCMC samples. All global parameter values had $\hat{R} \approx 1.00 \leq 1.10$ indicating
67 that chains are converged to the target distributions. The ESS of model parameters were typically
68 greater than 500 (out of 3200 total samples). The minimum ESS of global-parameters was 233
69 (on $v_{\epsilon, Low}$). Visual inspection of the parameters with smaller ESSs confirmed their convergence
70 to target distributions. We confirmed that changing both df (i.e. broadness of the tail) of the
71 Student's t prior distributions and sd of the Normal prior distributions did not change our findings.

72 **2.2 Parameter recovery test**

73 To assess the adequacy of the hierarchical Bayesian model-fitting method, we tested how well
74 the HBM could recover ‘true’ parameter values that were used to simulate synthetic data. We
75 simulated participants’ behaviour assuming that they behave according to the model with each
76 parameter setting. We generated ‘true’ parameter values for each simulated agent based on the
77 experimentally fit global parameters (Table 1 in the main text). We then simulated synthetic
78 behavioural data and recovered their parameter values using the HBM described above.

79 **2.3 Time-dependent conformity exponent $\theta_{i,t}$ model**

80 We also considered the possibility of the conformity exponent being time-dependent (i.e. $\theta_{i,t} =$
81 $\theta_{i,0}^* + \gamma_i t/70$). If the slope γ_i is positive (negative), the frequency-dependent bias increases (de-
82 creases) over time. In this model, there are 7 individual parameters; namely, α_i , $\beta_{i,0}^*$, ϵ_i , $\sigma_{i,0}^*$, δ_i ,
83 $\theta_{i,0}^*$ and γ_i . We fitted this model to the experimental data using the HBM described above.

84 2.4 Other figures related to the methods

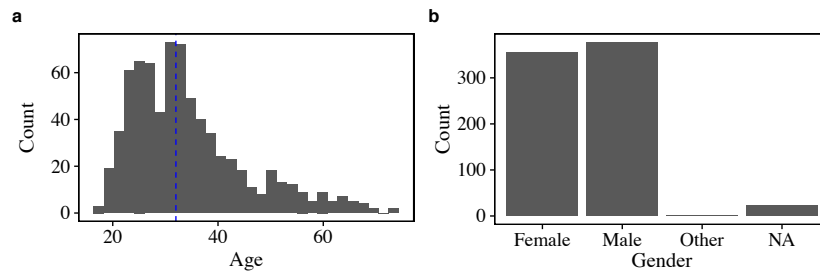


Figure S2. Histograms of the participants' age and gender. The mean age is indicated by a blue dashed line. Note that these data were inputted by participants themselves on the questionnaire forms.

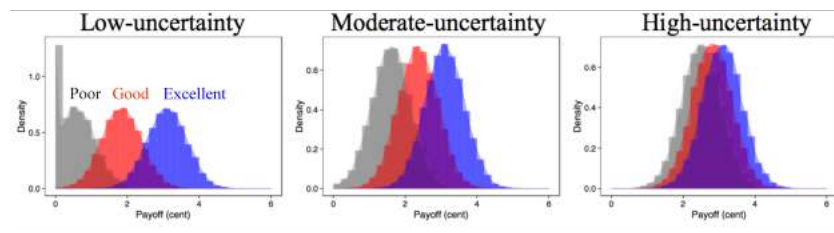


Figure S3. The distributions of payoffs generated by each of the slot machines for each condition. The poor, good and excellent slot are indicated by grey, red and blue, respectively. The payoff was truncated to zero if it would have been a negative value.

85 3 Appendix 3 Supplementary results

86 3.1 Individual-based simulation using other parameter sets

87 Individual-based model simulations using a different set of asocial learning parameters suggest
88 that our main findings from the simulation (Figure 1, 2 in the main text) are broadly robust in a
89 range of parameter combinations (Figure S4, S5, S6, S7).

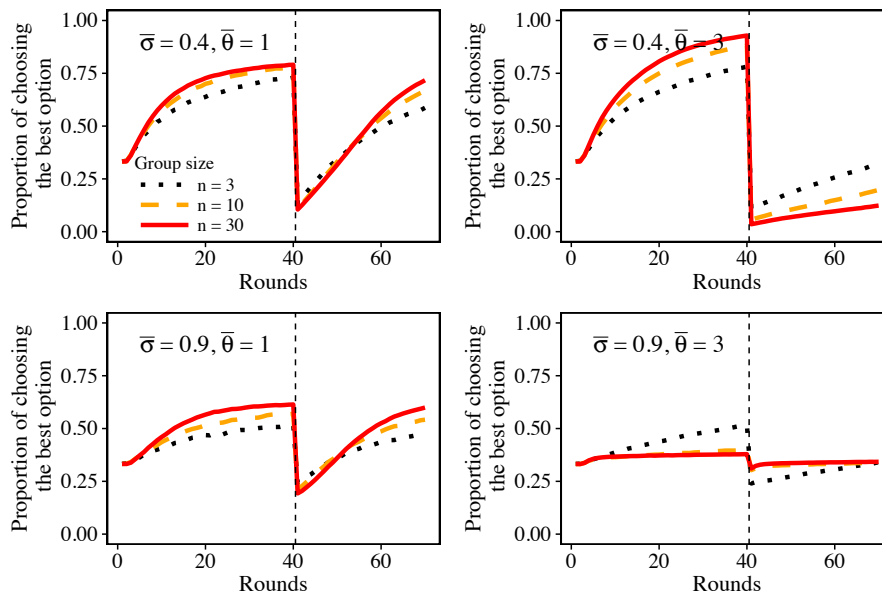


Figure S4. The same figure as Figure 1 in the main text, except for the asocial learning parameter settings (i.e.

$\mu_\alpha = 0.7, \mu_{\beta_0^*} = 2, \mu_\epsilon = 4, \nu_\alpha = 1, \nu_{\beta_0^*} = 1, \nu_\epsilon = 1, \nu_\sigma = 1, \text{ and } \nu_\theta = 1$).

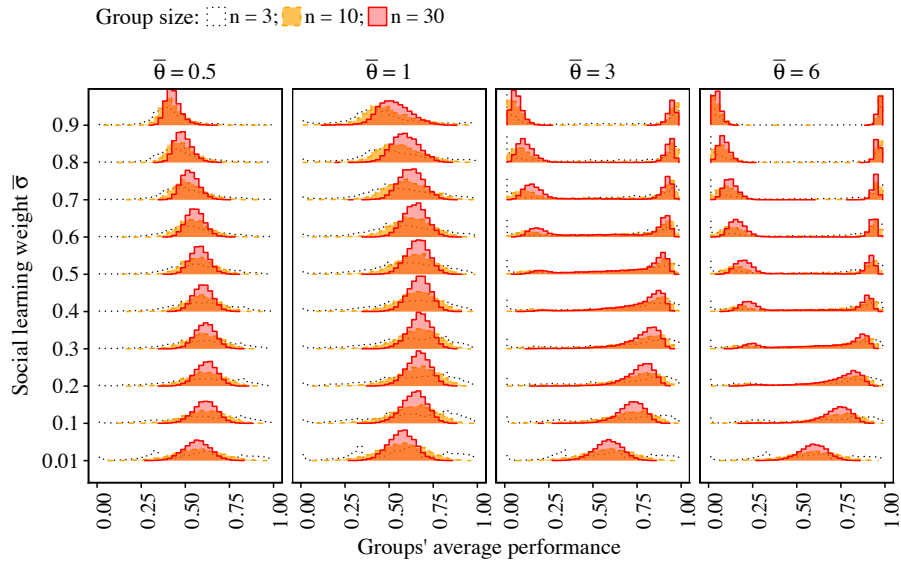


Figure S5. The same figure as Figure 2 in the main text, except for the asocial learning parameter settings.

Parameter values were the same in Figure S4.

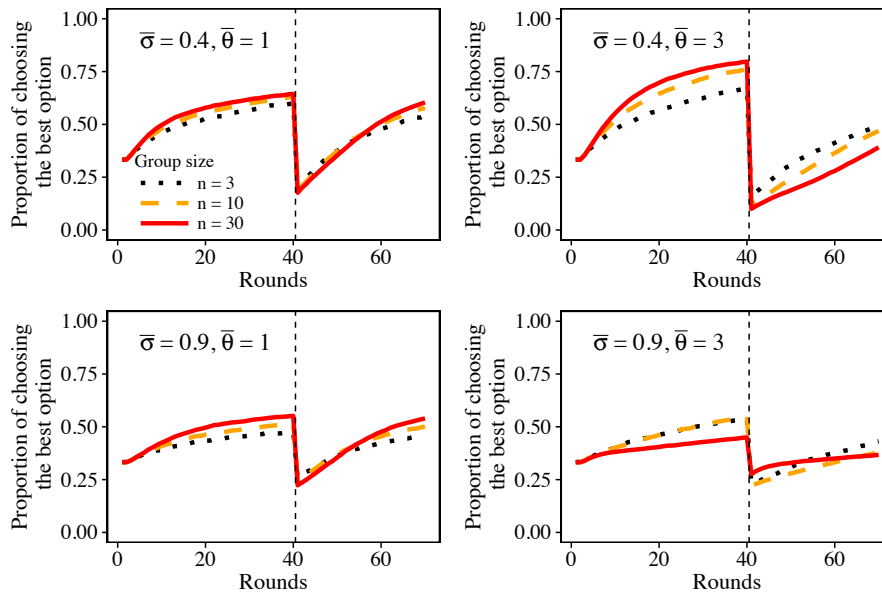


Figure S6. The same figure as Figure 1 in the main text, except for the asocial learning parameter settings (i.e.

$\mu_\alpha = 0.8, \mu_{\beta_0^*} = 0.5, \mu_\epsilon = 3, v_\alpha = 1, v_{\beta_0^*} = 2, v_\epsilon = 2, v_\sigma = 2,$ and $v_\theta = 2$).

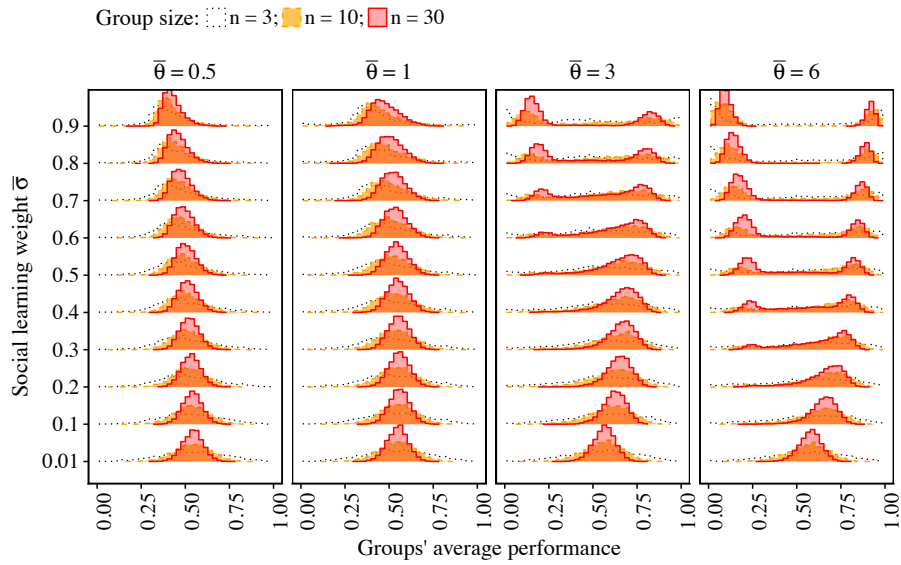


Figure S7. The same figure as Figure 2 in the main text, except for the asocial learning parameter settings.

Parameter values were the same in Figure S6.

90 3.2 Parameter recovery test

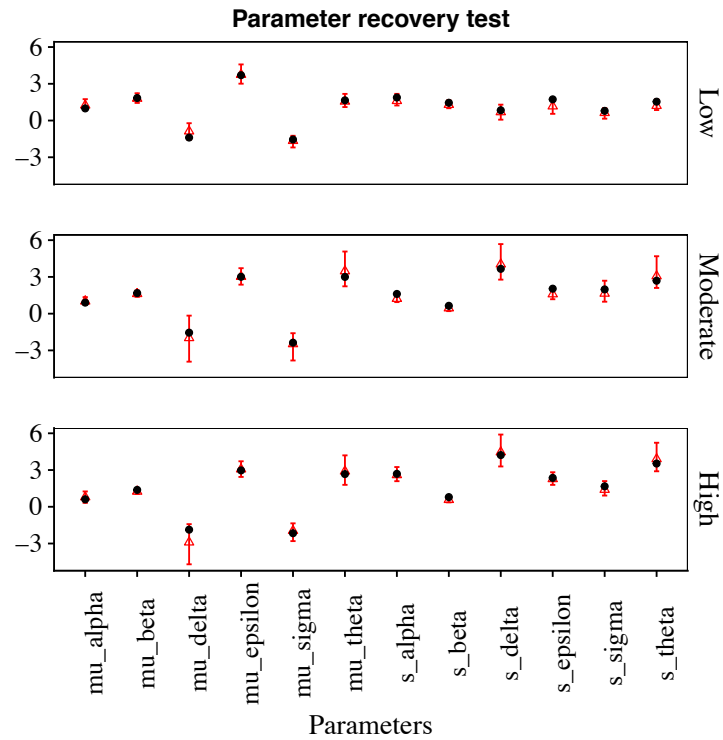


Figure S8. The parameter recovery performance on the global parameters. The black points are the true values and the red triangles are the mean posterior values (i.e. recovered values). The 95% Bayesian credible intervals are shown by the error bars.

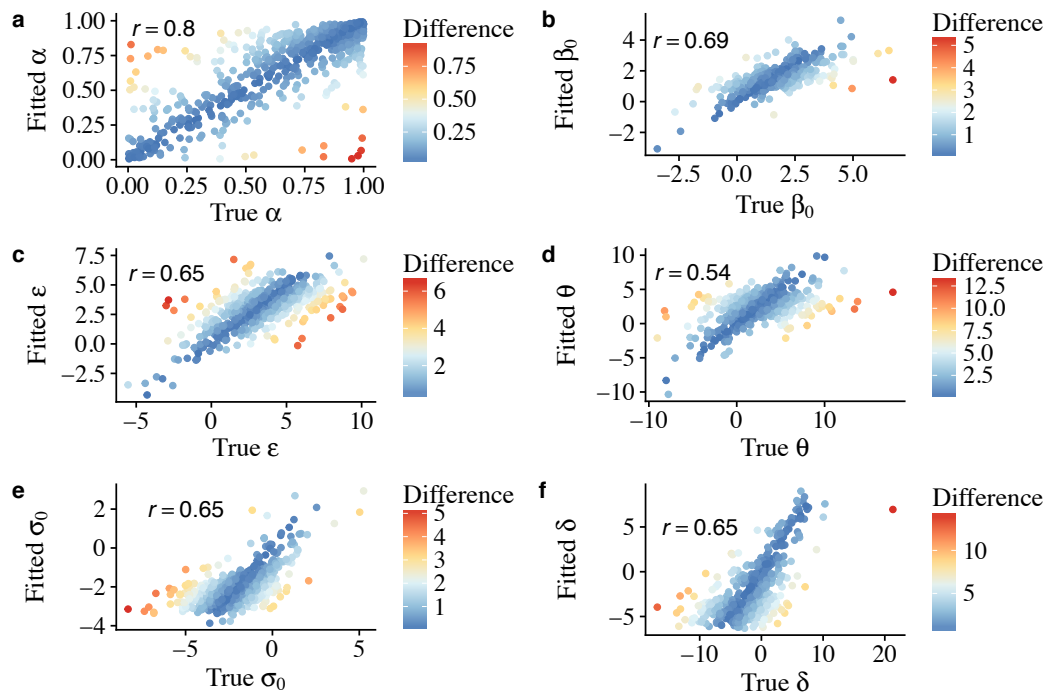


Figure S9. The parameter recovery performance on the individual parameters. The x-axis is the true value and the y-axis is the fitted (i.e. the mean posterior) value. The differences between the true value and the fitted value are shown in different colours. The correlation coefficients between the true value and the fitted value are shown.

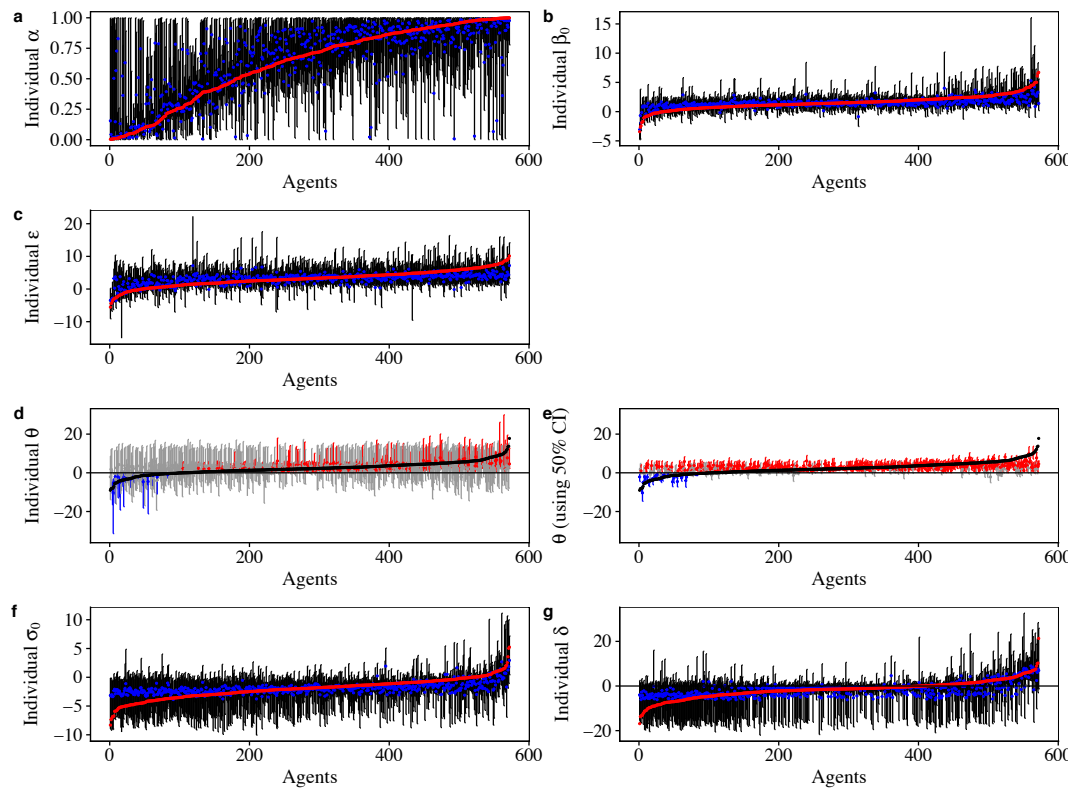


Figure S10. The parameter recovery performance on the individual parameters. (a,b,c,f,g) The red points are the true individual parameter values, the blue points are the mean posterior fitted values and the black lines are the 95% Bayesian CI. (d) The categorisation of three different strategies based on the 95% Bayesian CI and (e) on the 50% Bayesian CI of individual θ_i values. The red coloured individuals are categorised as the positive frequency-dependent copiers (positive frequency-biased choice), the blue coloured individuals are categorised as the negative frequency-dependent copiers (negative frequency-biased choice) and the grey individual are categorised as the asocial random copiers (nearly random decision-making). The black points are the true θ_i values. The horizontal lines indicate the categorisation threshold where $\theta_i = 0$.

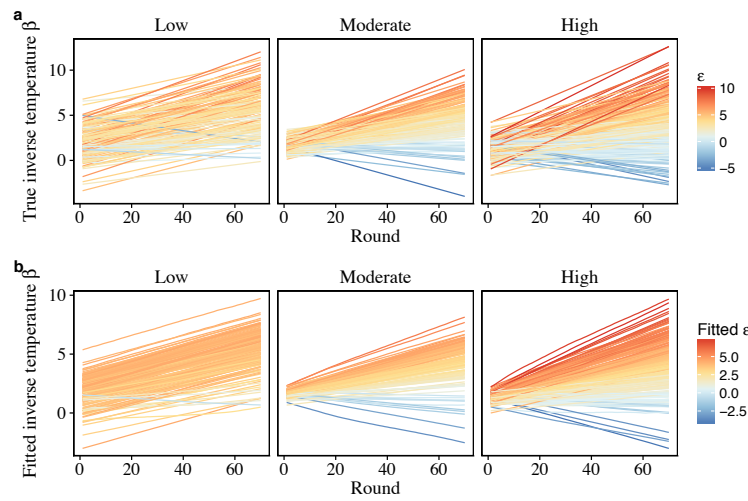


Figure S11. The temporal evolution of (a) the true individual *inverse temperature* $\beta_{i,t}$ parameters and (b) the recovered $\beta_{i,t}$ value. The magnitude of individual slope parameter ϵ_i are shown in different colours.

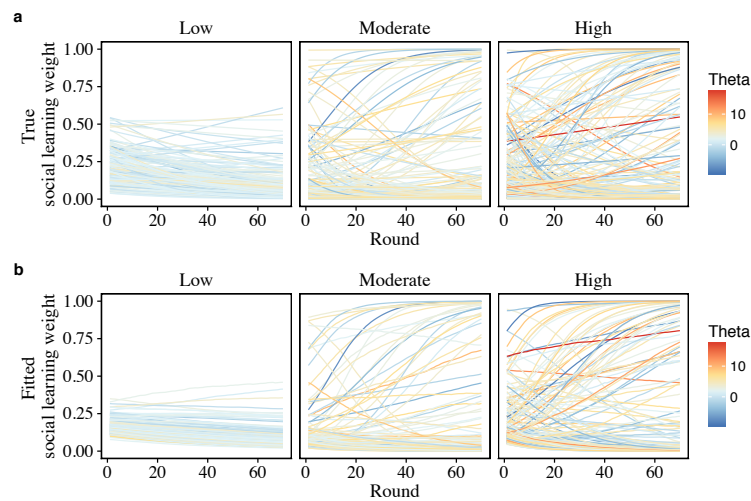


Figure S12. The temporal evolution of (a) the true individual *social learning weight* $\sigma_{i,t}$ parameters and (b) the recovered $\sigma_{i,t}$ value. The magnitude of individual conformity exponent θ_i are shown in different colours.

91 **3.3 Model fitting to our experimental data**

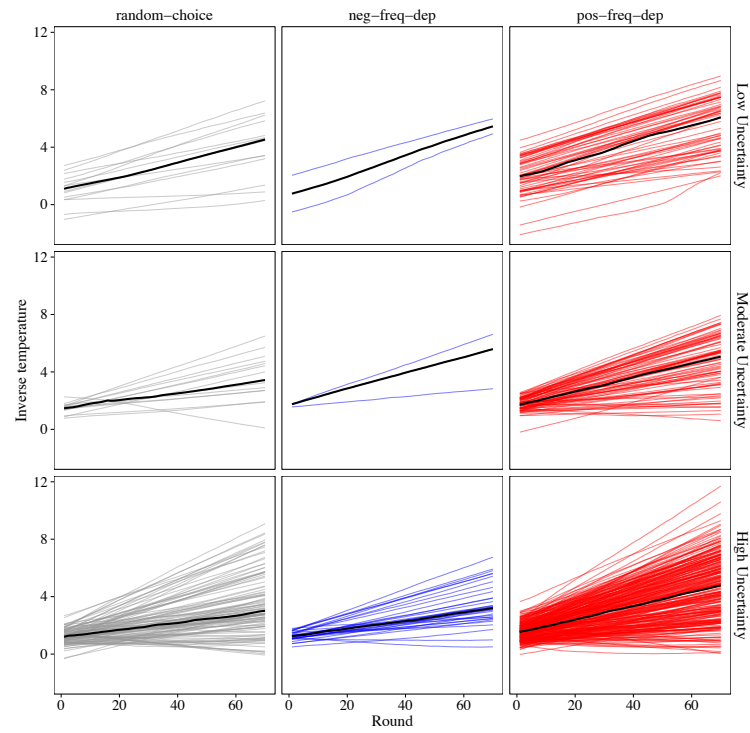


Figure S13. Individual inverse temperature $\beta_{i,t}$ fit for each experimental participant.

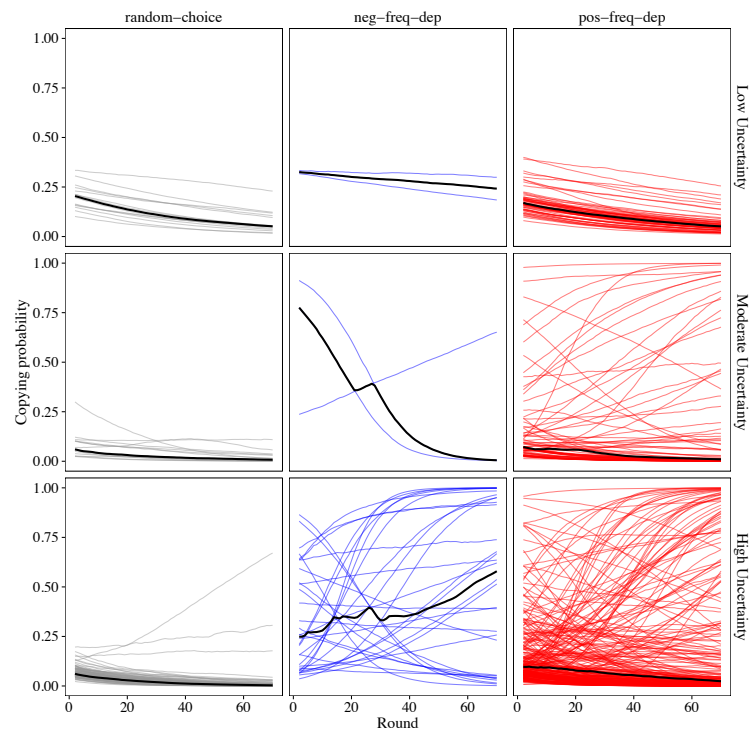


Figure S14. Individual social learning weights $\sigma_{i,t}$ fit for each experimental participant.

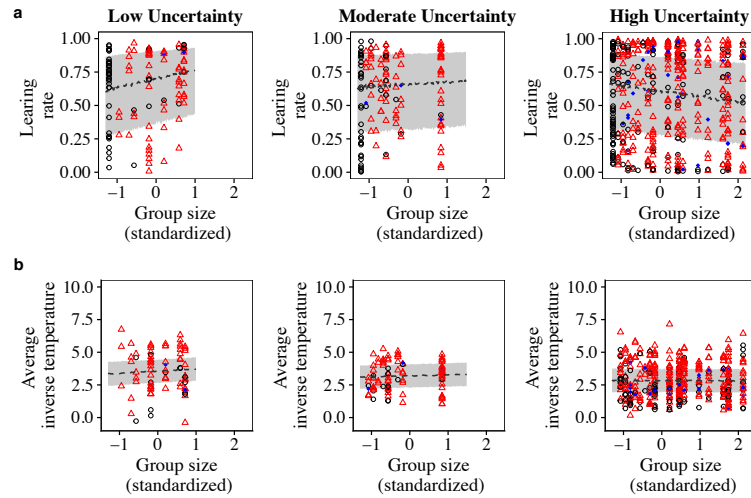


Figure S15. (a) Estimated learning rate α_i and (b) estimated mean inverse temperature $\bar{\beta}_i = (\sum_t \beta_{i,t})/70$ for each individual shown for each different learning strategy (red-triangle: positive frequency-biased choice, blue-diamond: negative frequency-biased choice; grey open circle: nearly random decision-making). Predictions from the fitted generalised mixed models are shown by dashed lines (the shaded areas indicate 50% Bayesian credible intervals).

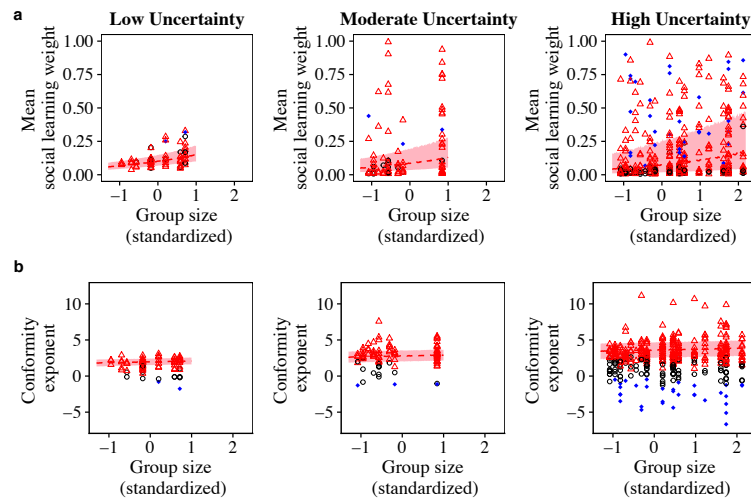


Figure S16. (a) Estimated social learning weight and (b) estimated conformity exponent for each individual shown for each different learning strategy (red-triangle: positive frequency-biased choice, blue-diamond: negative frequency-biased choice; grey open circle: nearly random decision-making). The dashed lines show regressions of the fitted generalised mixed models for only the positive frequency-biased choice individuals (the shaded areas indicate 50% Bayesian credible intervals).

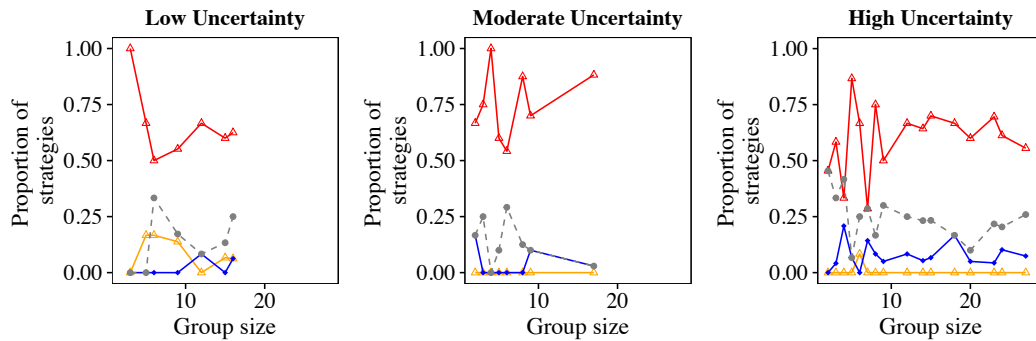


Figure S17. Model fitting for the three different task's uncertain conditions (the Low-, Moderate- and High-uncertainty) and the different group size. Frequencies of four different learning strategies are shown in different styles (red-triangle: strong positive frequency-dependent learning $\theta_i > 1$, orange-triangle: weak positive frequency-dependent learning $0 < \theta_i \leq 1$, blue-circle: negative frequency-dependent learning; grey-circle: nearly random choice strategy).

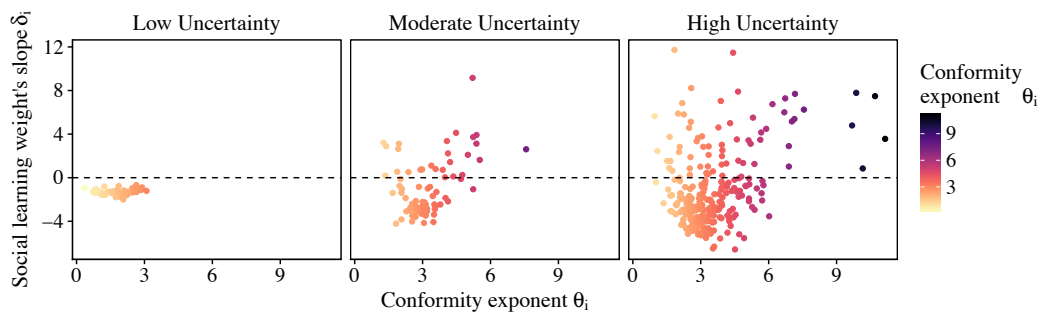


Figure S18. The relationship between θ_i and the slope of social learning weight δ_i . The horizontal dashed lines indicate a threshold at which $\sigma_{i,t}$ does not change with time (i.e. $\delta_i = 0$).

Table S1

The mean and the 95% Bayesian credible intervals of the posterior global variance parameters governing the magnitude of individual variations in each free parameter. The number of participants (N) for each experimental condition are also shown.

Parameters	Group condition						Solitary condition		
	Uncertainty			Uncertainty			Uncertainty		
	Low	Moderate	High	Low	Moderate	High	Low	Moderate	High
ν_{α^*} (learning rate)	1.88 [1.20, 2.82]	1.61 [1.14, 2.23]	2.69 [2.23, 3.21]	1.79 [0.98, 3.03]	2.37 [1.46, 3.58]	2.34 [1.39, 3.77]	1.79 [0.98, 3.03]	2.37 [1.46, 3.58]	2.34 [1.39, 3.77]
$\nu_{\beta_0^*}$ (inv. temp.)	1.45 [0.91, 2.16]	0.64 [0.34, 1.00]	0.79 [0.61, 1.00]	0.77 [0.42, 1.25]	0.96 [0.46, 1.61]	0.71 [0.40, 1.08]	0.77 [0.42, 1.25]	0.96 [0.46, 1.61]	0.71 [0.40, 1.08]
ν_{ϵ} (inv. temp.)	1.73 [0.41, 3.34]	2.04 [1.27, 2.96]	2.36 [1.89, 2.85]	1.75 [0.85, 2.94]	1.76 [0.85, 2.87]	2.23 [1.43, 3.08]	1.75 [0.85, 2.94]	1.76 [0.85, 2.87]	2.23 [1.43, 3.08]
$\nu_{\sigma_0^*}$ (soc. wight)	0.79 [0.17, 1.50]	1.98 [1.17, 3.15]	1.67 [1.26, 2.18]	-	-	-	-	-	-
ν_{δ} (soc. wight)	0.84 [0.05, 1.94]	3.66 [1.92, 5.78]	4.22 [3.30, 5.40]	-	-	-	-	-	-
ν_{θ} (conformity coeff.)	1.54 [0.87, 2.61]	2.69 [1.60, 4.32]	3.53 [2.67, 4.65]	-	-	-	-	-	-
N	77	98	398	36	34	56	36	34	56

92 **3.4 Results of a time-dependent conformity model ($\theta_{i,t}$)**

93 **3.4.1 Parameter recovery test**

94 The parameter recovery test showed that the all true global parameter values were fallen into the
95 95% Bayesian credible interval (Figure S19). Correlations between individual true parameters
96 and recovered parameters were all positive, while the correlation coefficients of both $\theta_{i,0}^*$ and γ_i
97 were lower than other parameters (Figure S20). At least 89% of the true individual parameter
98 values were correctly recovered (i.e. 97% of α_i , 96% of $\beta_{i,0}^*$, 97% of ϵ_i , 96% of $\sigma_{i,0}^*$, 94% of δ_i ,
99 96% of $\theta_{i,0}^*$ and 89% of γ_i were fallen into the 95% Bayesian CI; Figure S21).

100 Figure S22, S23 and S24 show that overall patterns of temporal dynamics of these parameters
101 were well recovered.

102 **3.4.2 Fitting to our experimental data**

103 In order to compared the findings from the time-independent θ_i model (see Results section in
104 the main text), we again categorized the participants as deploying three different learning strate-
105 gies based on their mean fitted conformity exponent values; namely, the ‘positive frequency-
106 dependent copying’ strategy ($\bar{\theta}_i \gg 0$), the ‘negative-frequency dependent copying’ strategy
107 ($\bar{\theta}_i \ll 0$) and the ‘random choice’ strategy ($\bar{\theta}_i \approx 0$). Note, the conformity exponent here is
108 averaged over time: $\bar{\theta}_i = (\sum_t \theta_{i,t})/70$. Figure S25 suggests that the patterns were consistent with
109 Figure 3 in the main text, and hence our conclusion was not changed.

110 Individual frequency dependence changed over time (Figure S26). The conformity exponents
111 generally increased with experimental round, while some individuals in the High-uncertain con-

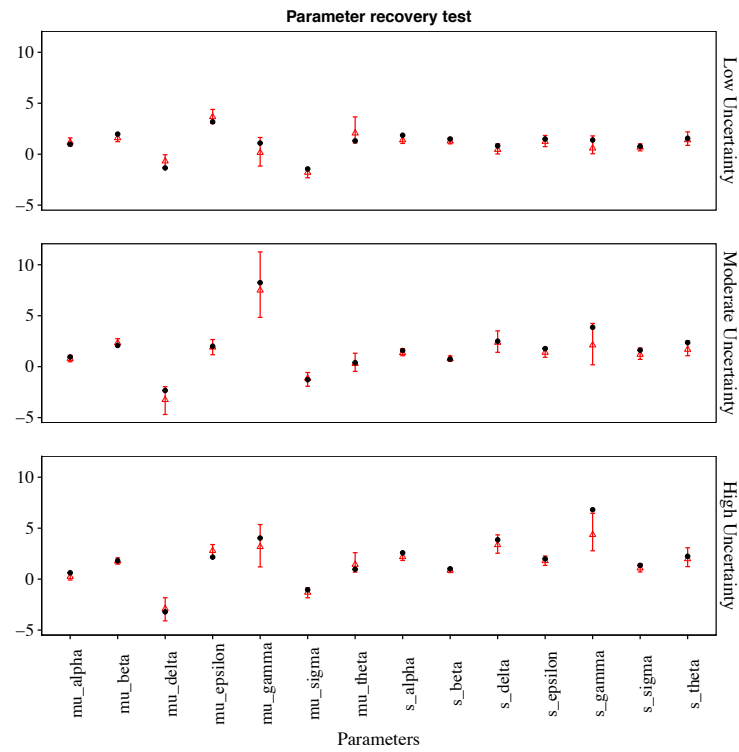


Figure S19. The parameter recovery performance on the global parameters. The black points are the true values and the red triangles are the mean posterior values (i.e. recovered values). The 95% Bayesian credible intervals are shown by the error bars.

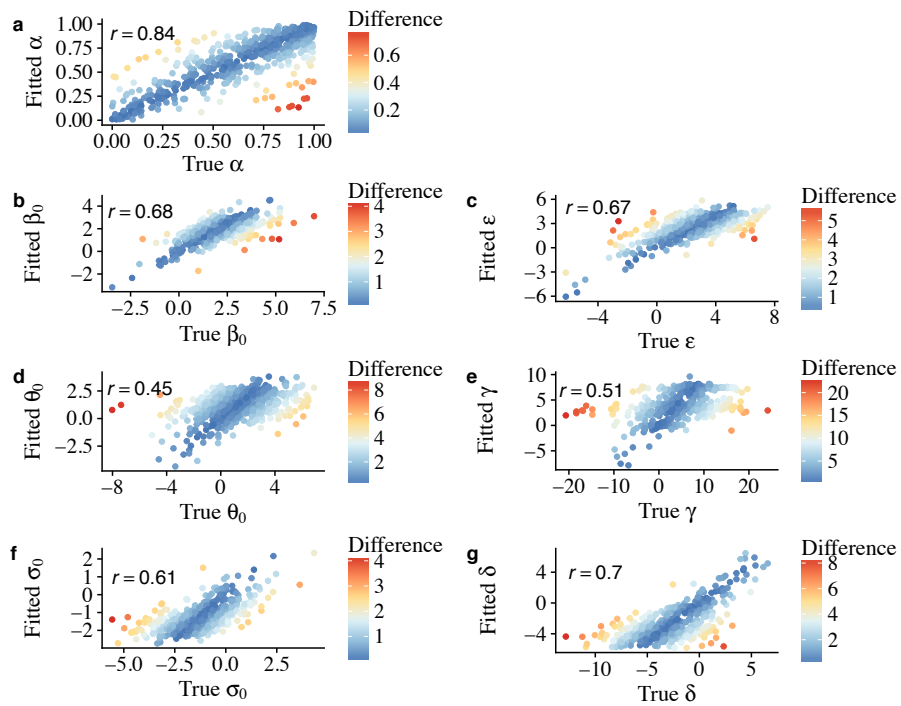


Figure S20. The parameter recovery performance on the individual parameters. The x-axis is the true value and the y-axis is the fitted (i.e. the mean posterior) value. The differences between the true value and the fitted value are shown in different colour. The correlation coefficients between the true value and the fitted value are shown.

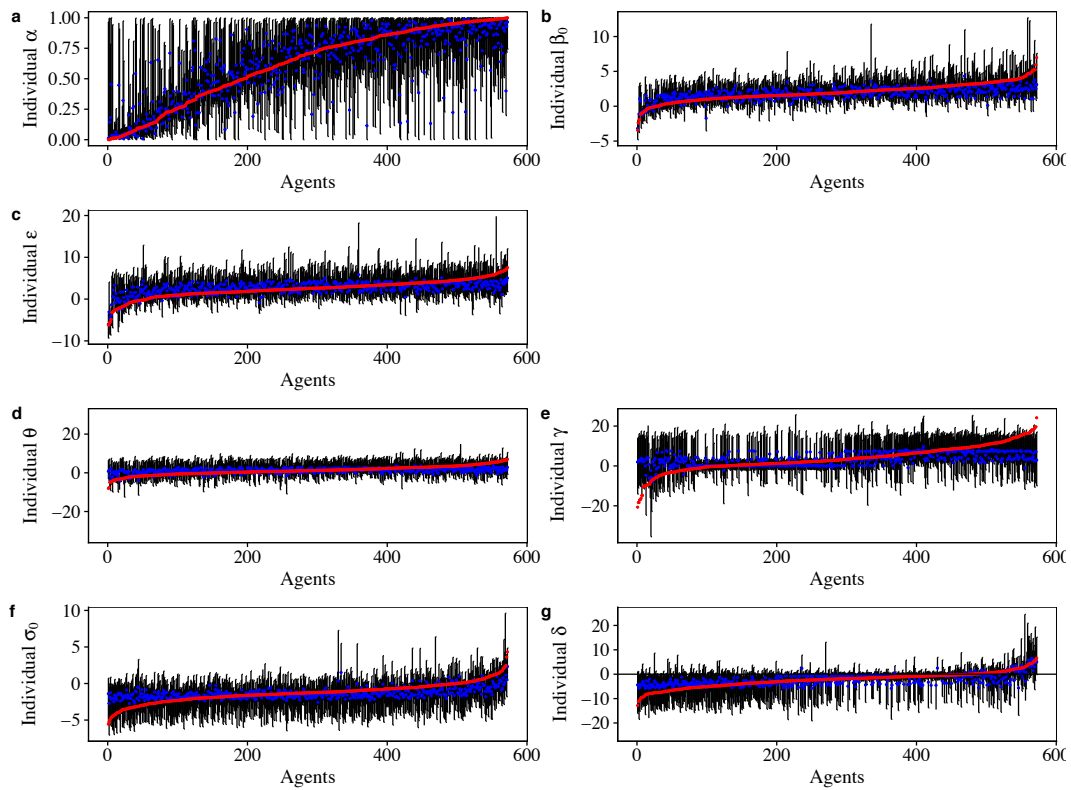


Figure S21. The parameter recovery performance on the individual parameters. (a,b,c,e,g) The red points are the true individual parameter values, the blue points are the mean posterior fitted values and the black lines are the 95% Bayesian CI. (d) The categorisation of three different strategies based on the 95% Bayesian CI and (e) on the 50% Bayesian CI of individual θ_i values. The red coloured individuals are categorised as the positive frequency-dependent copiers (positive frequency-biased choice), the blue coloured individuals are categorised as the negative frequency-dependent copiers (negative frequency-biased choice) and the grey individual are categorised as the asocial random copiers (nearly random decision-making). The black points are the true θ_i values. The horizontal lines indicate the categorisation threshold where $\theta_i = 0$.

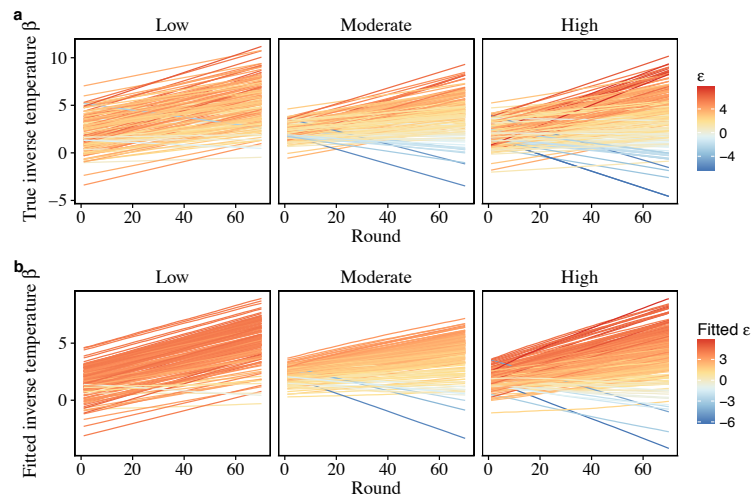


Figure S22. The temporal evolution of (a) the true individual *inverse temperature* $\beta_{i,t}$ parameters and (b) the recovered $\beta_{i,t}$ value. The magnitude of individual slope parameter ϵ_i are shown in different colours.

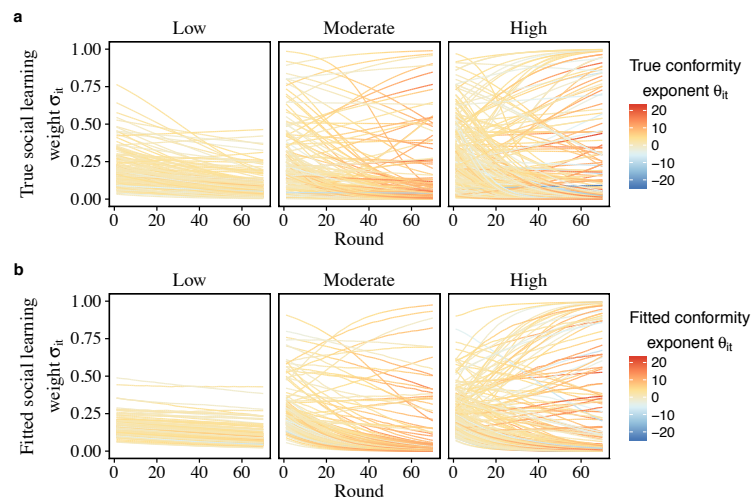


Figure S23. The temporal evolution of (a) the true individual *social learning weight* $\sigma_{i,t}$ parameters and (b) the recovered $\sigma_{i,t}$ value. The magnitude of individual conformity exponent θ_i are shown in different colours.

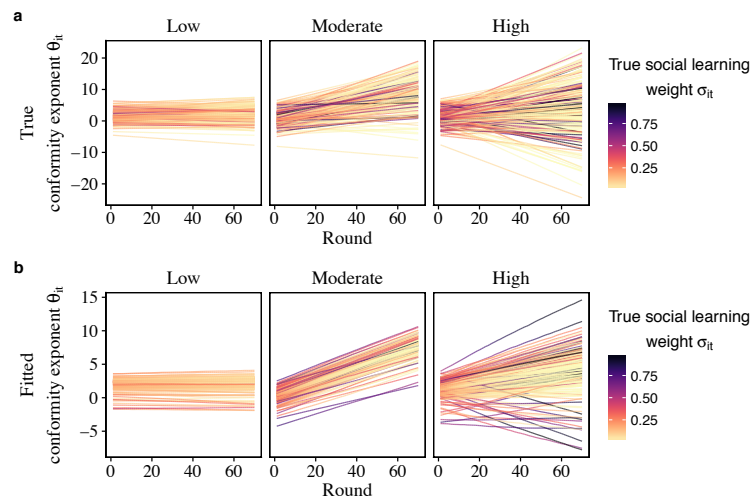


Figure S24. The temporal evolution of (a) the true and (b) the recovered individual *conformity exponent* $\theta_{i,t}$ value. The magnitude of individual social learning weights $\sigma_{i,t}$ are shown in different colours.

112 ditions decreased rather than accelerated their frequency dependence over time. However, note
113 that the fitting of slope parameter γ_i was relatively unreliable (i.e. only 89% of individual param-
114 eters were recovered correctly). Extensive variation in both the social learning weigh $\sigma_{i,t}$ and
115 the conformity exponent $\theta_{i,t}$ found in high-uncertain circumstances are consistent with the main
116 findings (Figure 3g-i, Figure 4a-c).

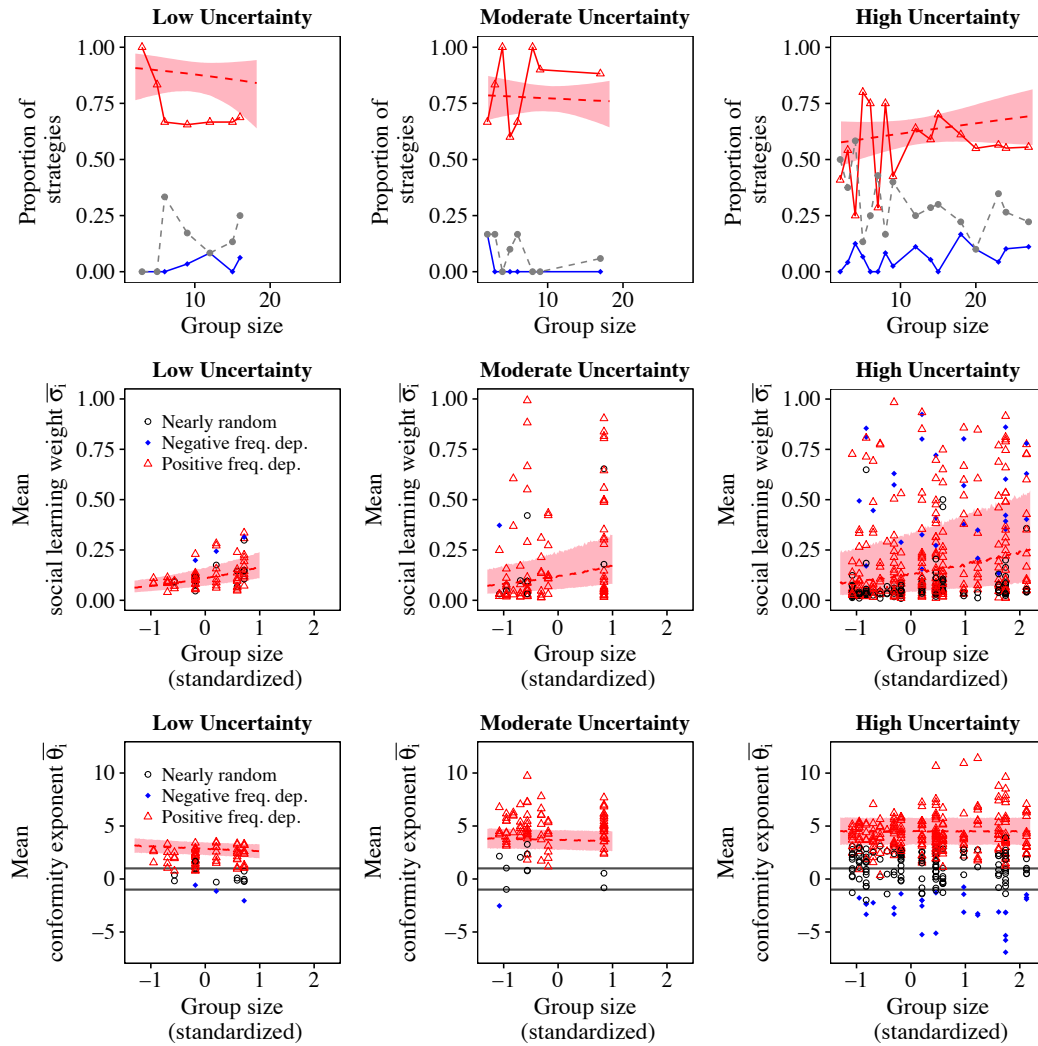


Figure S25. Model fitting for the three different task uncertainty conditions (the Low-, Moderate- and High-uncertainty) and the different group size. Three different learning strategies are shown in different styles (red-triangle: positive frequency-dependent learning, blue-circle: negative frequency-dependent learning; grey-circle: nearly random choice strategy). Note, we averaged individual conformity exponent $\theta_{i,t}$ over time to categorise individual strategies. (Top row) Frequencies of three different learning strategies. (Middle row) Estimated social learning weight, and (Bottom row) estimated mean conformity exponent, for each individual shown for each learning strategy. The 50% Bayesian CIs of the fitted GLMMs are shown by dashed lines and shaded areas. The horizontal lines in (g-i) show a region $-1 < \bar{\theta}_i < 1$.

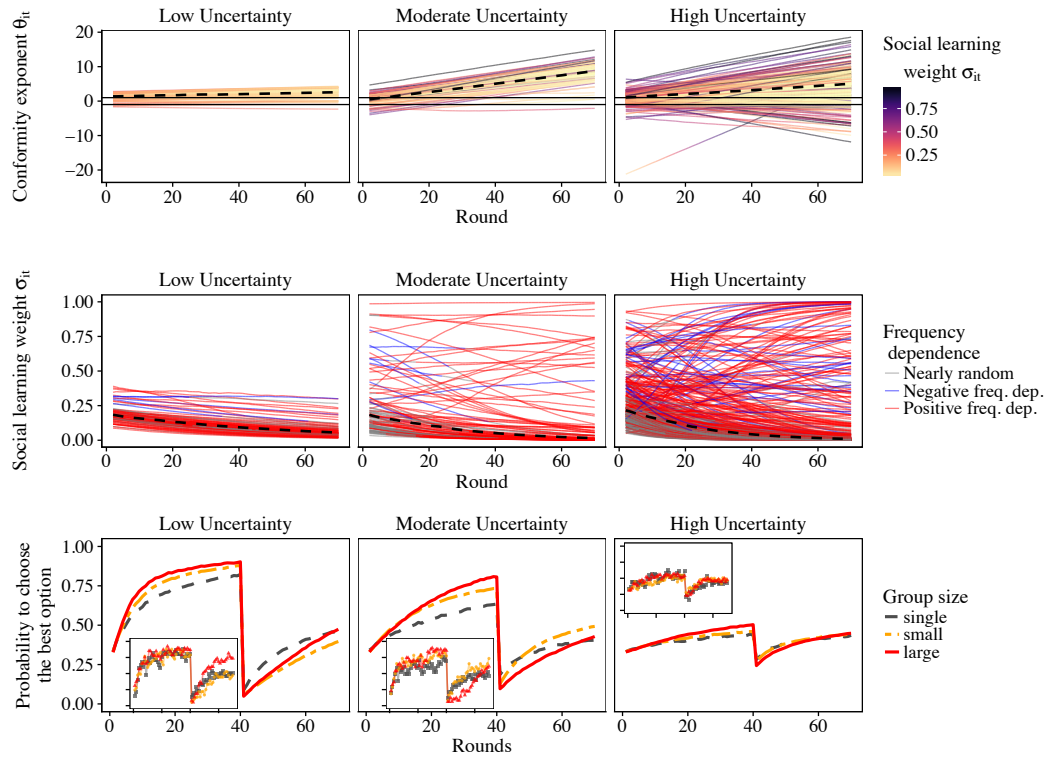


Figure S26. Change in fitted values (i.e. median of the Bayesian posterior distribution) of (Top row) the conformity exponent $\theta_{i,t}$ and (Middle row) the social learning weight $\sigma_{i,t}$ with time for each individual, for each level of task uncertainty. Thick dashed lines are the median values across the subjects for each uncertainty condition. (Bottom row) Change in average decision accuracy of the individual-based post-hoc model simulations using the experimentally fit parameter values of the alternative model (main panels). The inner panels show the average decision accuracies of the experimental participants. Each line indicates different group-size categories (red-solid: large groups, orange-halfdashed: small groups, grey-dashed: lone individuals). All individual performances were averaged within the same size category. The large or small groups were categorised using the median sizes for each experimental condition, i.e. small groups were: $n \leq 9$, $n \leq 6$ and $n \leq 11$ for the Low-, Moderate- and High-uncertain conditions, respectively.

117 3.5 Statistical analyses for the experimental data

Table S2

Mean and the 95% Bayesian credible intervals of the fixed effects in the GLMM predicting the probability to become a positive frequency-dependent copier. The sized effects whose CI are either below or above zero (i.e. significant) are shown in bold face.

Effect	2.5%	50%	97.5%	Effective sample size	Rhat
β_1 (intercept)	1.05	1.71	2.50	667	1.01
β_2 (group size)	-0.94	-0.05	0.87	2744	1.00
β_3 (uncertainty)	-1.88	-1.02	-0.25	1548	1.00
β_4 (age)	-0.12	0.43	1.10	925	1.01
β_5 (gender)	-1.06	-0.13	0.84	3154	1.00
β_6 (size*uncrtn)	-0.72	0.24	1.19	2880	1.00
β_7 (size*age)	-0.16	0.08	0.32	1869	1.01
β_8 (size*gndr)	-0.37	0.03	0.44	4875	1.00
β_9 (uncrtn*age)	-1.46	-0.73	-0.15	3167	1.00
β_{10} (uncrtn*gndr)	-1.10	0.02	1.09	3661	1.00
β_{11} (age*gndr)	-0.39	-0.02	0.37	2712	1.00

Table S3

Mean and the 95% Bayesian credible intervals of the fixed effects in the GLMM predicting individual parameter values of the social learning weight $\bar{\sigma}_i$. The sized effects whose CI are either below or above zero (i.e. significant) are shown in bold face.

Effect	2.5%	50%	97.5%	nEff	Rhat
β_1 (intercept)	-2.32	-2.09	-1.84	4959	1.00
β_2 (group size)	0.15	0.52	0.93	5230	1.00
β_3 (uncertainty)	-0.98	-0.59	-0.22	4784	1.00
β_4 (age)	-0.36	-0.18	-0.02	2126	1.00
β_5 (gender)	-0.45	-0.16	0.13	4513	1.00
β_6 (size*uncrtn)	-0.57	-0.10	0.34	5440	1.00
β_7 (size*age)	-0.19	-0.02	0.14	5359	1.00
β_8 (size*gndr)	-0.32	-0.01	0.30	4127	1.00
β_9 (uncrtn*age)	-0.17	0.07	0.32	4088	1.00
β_{10} (uncrtn*gndr)	-0.37	0.12	0.62	4205	1.00
β_{11} (age*gndr)	-0.09	0.12	0.35	4963	1.00
γ (uncertainty effect on variance)	1.11	1.38	1.62	3067	1.00

Table S4

Mean and the 95% Bayesian credible intervals of the fixed effects in the GLMM predicting the social learning weight $\bar{\sigma}_i$ for the positive frequency-biased choice individuals only. The sized effects whose CI are either below or above zero (i.e. significant) are shown in bold face.

Effect	2.5%	50%	97.5%	nEff	Rhat
β_1 (intercept)	-2.42	-2.17	-1.91	5601	1.00
β_2 (group size)	0.09	0.47	0.90	4509	1.00
β_3 (uncertainty)	-0.75	-0.28	0.17	6011	1.00
β_4 (age)	-0.33	-0.14	0.04	5796	1.00
β_5 (gender)	-0.36	-0.03	0.30	6075	1.00
β_6 (size*uncrtn)	-0.55	-0.01	0.49	5410	1.00
β_7 (size*age)	-0.27	-0.06	0.14	6022	1.00
β_8 (size*gndr)	-0.42	-0.05	0.33	6174	1.00
β_9 (uncrtn*age)	-0.36	-0.04	0.29	6483	1.00
β_{10} (uncrtn*gndr)	-0.75	-0.13	0.49	4746	1.00
β_{11} (age*gndr)	-0.16	0.10	0.36	5927	1.00
γ (uncertainty effect on variance)	1.14	1.50	1.80	5729	1.00

Table S5

Mean and the 95% Bayesian credible intervals of the fixed effects in the GLMM predicting individual parameter values of the conformity exponent θ_i . The sized effects whose CI are either below or above zero (i.e. significant) are shown in bold face.

Effect	2.5%	50%	97.5%	nEff	Rhat
β_1 (intercept)	1.30	1.64	2.01	2571	1.00
β_2 (group size)	-0.69	-0.17	0.35	5443	1.00
β_3 (uncertainty)	0.38	0.90	1.41	2602	1.00
β_4 (age)	-0.19	0.07	0.33	2967	1.00
β_5 (gender)	-0.34	0.10	0.54	3557	1.00
β_6 (size*uncrtn)	-0.40	0.19	0.79	5317	1.00
β_7 (size*age)	-0.27	-0.06	0.14	5172	1.00
β_8 (size*gndr)	-0.24	0.13	0.50	5167	1.00
β_9 (uncrtn*age)	-0.59	-0.26	0.07	3436	1.00
β_{10} (uncrtn*gndr)	-0.86	-0.21	0.45	3509	1.00
β_{11} (age*gndr)	-0.30	-0.02	0.27	4885	1.00
γ (uncertainty effect on variance)	1.07	1.31	1.54	4178	1.00

Table S6

Mean and the 95% Bayesian credible intervals of the fixed effects in the GLMM predicting the conformity exponent θ_i for the positive frequency-biased choice individuals only. The sized effects whose CI are either below or above zero (i.e. significant) are shown in bold face.

Effect	2.5%	50%	97.5%	nEff	Rhat
β_1 (intercept)	1.74	2.00	2.29	4922	1.00
β_2 (group size)	-0.40	0.03	0.42	5695	1.00
β_3 (uncertainty)	1.20	1.64	1.04	4381	1.00
β_4 (age)	-0.32	-0.13	0.05	6046	1.00
β_5 (gender)	-0.40	-0.07	0.26	5988	1.00
β_6 (size*uncrtn)	-0.47	0.00	0.50	4458	1.00
β_7 (size*age)	-0.24	-0.07	0.11	5716	1.00
β_8 (size*gndr)	-0.12	0.19	0.51	5349	1.00
β_9 (uncrtn*age)	-0.15	0.10	0.37	6424	1.00
β_{10} (uncrtn*gndr)	-0.53	-0.01	0.51	5710	1.00
β_{11} (age*gndr)	-0.14	0.09	0.33	6545	1.00
γ (uncertainty effect on variance)	0.71	0.91	1.10	6545	1.00

Table S7

Mean and the 95% Bayesian credible intervals of the fixed effects in the GLMM predicting individual parameter values of the learning rate α_i . The sized effects whose CI are either below or above zero (i.e. significant) are shown in bold face.

Effect	2.5%	50%	97.5%	nEff	Rhat
β_1 (intercept)	0.12	0.67	1.23	4887	1.00
β_2 (group size)	-0.49	0.24	0.96	5413	1.00
β_3 (uncertainty)	-0.93	-0.27	0.38	4827	1.00
β_4 (age)	-0.48	-0.03	0.40	5794	1.00
β_5 (gender)	-0.40	0.38	1.17	4908	1.00
β_6 (size*uncrtn)	-1.24	-0.48	0.29	5423	1.00
β_7 (size*age)	-0.25	-0.04	0.17	6157	1.00
β_8 (size*gndr)	-0.25	0.15	0.54	6305	1.00
β_9 (uncrtn*age)	-0.09	0.38	0.85	6085	1.00
β_{10} (uncrtn*gndr)	-1.21	-0.29	0.65	4699	1.00
β_{11} (age*gndr)	-0.35	-0.01	0.34	5824	1.00

Table S8

Mean and the 95% Bayesian credible intervals of the fixed effects in the GLMM predicting individual parameter values of the average inverse temperature $\bar{\beta}_i$. The sized effects whose CI are either below or above zero (i.e. significant) are shown in bold face.

Effect	2.5%	50%	97.5%	nEff	Rhat
β_1 (intercept)	3.09	3.47	3.85	5906	1.00
β_2 (group size)	-0.48	0.03	0.54	5707	1.00
β_3 (uncertainty)	-0.87	-0.43	0.02	5863	1.00
β_4 (age)	-0.49	-0.21	0.08	4498	1.00
β_5 (gender)	-0.35	0.16	0.67	5845	1.00
β_6 (size*uncrtn)	-0.73	-0.17	0.37	5503	1.00
β_7 (size*age)	-0.20	-0.06	0.08	6454	1.00
β_8 (size*gndr)	0.02	0.26	0.50	6492	1.00
β_9 (uncrtn*age)	0.01	0.33	0.63	6167	1.00
β_{10} (uncrtn*gndr)	-1.19	-0.58	0.02	5718	1.00
β_{11} (age*gndr)	-0.33	-0.10	0.12	5558	1.00